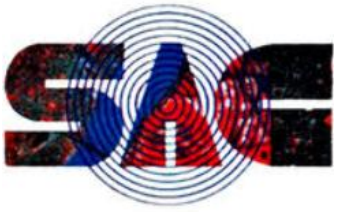

Design & Analysis of a Compact Ultra-Wideband Microstrip Bandpass Filter Centered at 3.825 GHz

Report submitted for completion of training
(Microwave Remote Sensing Area)
Program of Space Applications Centre

Submitted by:
KRISHANU BANDYOPADHYAY
Student ID- **16900321125**
B Tech (Electrical & Electronics Engineering)

Under the Guidance of:
SRI. VINIT KUMAR
SCI/ENGR-SG
MSRD/MSRG/MRSA
Space Application Centre(ISRO),Ahmedabad

Institution**:**
Academy of Technology (AOT)
Maulana Abul Kalam Azad Institute of Technology (MAKAUT)
West Bengal

SRTD-RTCG-MISA
Space **A**pplications **C**entre (ISRO)
Ahmedabad, Gujrat
03/03/2025 to 20/05/2025

ACKNOWLEDGEMENT

I would like to express my profound gratitude to all those who contributed to the successful completion of this project.

Firstly, I would like to express my gratitude towards **Smt. Harshita Tolani,** Head, MSRD, MSRG, MRSA for letting me work under her division and dive into the domain of rf/microwave.

I am especially indebted to my guide, **Sri Vinit Kumar**, whose expert guidance, constructive feedback, and unwavering support were instrumental throughout the duration of this work. Their insights and encouragement have been invaluable.

I would also like to extend my sincere thanks to the other supportive personals, **Dr. Anamiya Bhattacharya**, **Sri Vivan Prakash**, **Sri Prashant**, **Smt. Shrija Bhattacharya**, whose assistance, and constant support made everything seem approachable for me.

My appreciation also goes to my peers and colleagues, **Sri Abhay Kumar Nathani**, **Sri Akshat Srivastava**, **Smt. Nisha Bagadia** for their helpful discussions, collaboration, and moral support, which played a significant role in overcoming challenges during this endeavour.

Finally, I am deeply grateful to my family for their patience, understanding, and continued encouragement, without which this work would not have been possible.

ABSTRACT

The project titled "**Design & Analysis of a Compact Ultra-Wideband Microstrip Bandpass Filter Centered at 3.825 GHz**" focuses on the theoretical development and the design of microstrip bandpass filter suitable for the C&S-Band application. Filters are crucial in the domain of satellite communication systems, radar systems, and various other systems. Filters can both be realised in the form of lumped components or in the form of distributive components. This project report aims to develop an microstrip filter that meets the stringent performance criteria while ensuring the satisfaction of the provided specifications.

The design and implementation of microstrip bandpass filters play a critical role in the development of modern communication systems, particularly for **ultra-wideband (UWB)** applications. This report explores the design of a compact microstrip bandpass filter operating in the UWB frequency range, **centred at 3.825 GHz**, with a bandwidth of **2.4 GHz**, covering the passband from **2.625 GHz to 5.025 GHz**. The filter is designed to achieve high performance with low insertion loss, minimal return loss, and a **0.3 dB ripple** response, making it suitable for a variety of RF communication systems.

In addition, the design is constrained to a compact area of 1-inch × 1-inch, ensuring its applicability in space-limited environments. The use of high-dielectric substrates and precise electromagnetic simulations allows for optimization of the filter's electrical and physical characteristics. The resulting filter meets the stringent requirements for UWB communication systems, providing a robust solution for modern wireless applications that demand wide frequency coverage, low loss, and high selectivity. This work also discusses the design challenges associated with achieving such performance under physical and manufacturing constraints.

Contents

List of Figures:

CHAPTER-1

CHAPTER-2

CHAPTER-3

CHAPTER-4

List of Tables:

INTRODUCTION

In the rapidly evolving landscape of modern wireless communication systems, the demand for high-performance components such as **filters** has seen a sharp increase. Filters play a fundamental role in the design of communication systems by selectively allowing signals within a specified frequency range to pass through while blocking unwanted frequencies. Among various types of filters, **band pass filters** are crucial in **RF** (Radio Frequency) and **microwave** applications, where they are used to isolate desired frequency bands from the surrounding noise and interference. With the rise of **Ultra-Wideband (UWB)** communication systems, which require broad frequency coverage and minimal interference, the role of high-performance filters has become even more prominent. These systems, which operate over a wide range of frequencies, demand filters that can provide excellent performance, even at higher frequencies, while maintaining compactness and integration capabilities.

Ultra-Wideband (UWB) communication systems are a class of systems that operate over a very large frequency range, typically spanning from **3.1 GHz to 10.6 GHz** in most commercial applications. However, UWB technologies can also extend beyond these ranges, offering high data rates, low power consumption, and high-resolution sensing capabilities. UWB systems have found widespread applications in areas like **wireless personal area networks (WPANs)**, **radar** and **positioning systems**, as well as in **medical imaging** and **sensor networks**. The inherent advantage of UWB systems lies in their ability to transmit large amounts of data over short distances with minimal interference, making them ideal for both **high-speed communication** and **precision timing applications**.

Despite these advantages, UWB systems come with their own set of challenges. The wide frequency spectrum over which these systems operate requires filters that can provide high selectivity and low insertion loss, particularly over a broad passband. The filter must effectively reject signals outside the desired frequency range, ensuring that the communication signal is clear and free of interference. Additionally, with the increasing demand for portable and compact devices, it is necessary for these filters to be **small** yet highly efficient.

In this report we are going to build up the required theoretical knowledge and the development of such a particular UWB filter catering to the needs for various high frequency communication systems.

CHAPTER-1: BASICS CONCEPTS OF FILTERS

A filter is a two-port network used to control the frequency response of a certain point in an RF or microwave system by providing transmission at frequencies within the passband of the filter and attenuation in the stopband of the filter. Typical filter responses include low-pass, high-pass, band pass, and band-reject characteristics. Applications can be found in virtually any type of RF or microwave communication, radar, or test and measurement system.

This chapter describes basic concepts and theories that form the foundation for design of general RF/microwave filters.

1.1 Transfer Functions

General Definition: The transfer function of a two-port filter network is a mathematical description of network response characteristics, namely, a mathematical expression of S_{21}. On many occasions, an amplitude-squared transfer function for a lossless passive filter network is defined as

$$|S_{21}(j\Omega)|^2 = \frac{1}{1 + \varepsilon^2 F_n^2(\Omega)}$$

Where,

ε: Ripple constant.
$F_n(\Omega)$: Filtering or characteristic function.
Ω: Frequency variable (radian frequency variable of a low pass prototype filter with cut-off frequency at $\Omega = \Omega_c$ for $\Omega_c = 1$ rad/s)

For linear, time-invariant networks, the transfer function may be defined as a rational function, that is

$$S_{21}(p) = \frac{N(p)}{D(p)}$$

Where, N(p) and D(p) are polynomials in a complex frequency variable $p= \sigma+j\Omega$. For lossless passive network, the neper frequency is 0 and $p=j\Omega$.

For a given transfer function, the insertion loss response of the filter is given by:

$$L_A(\Omega) = 10 \log \frac{1}{|S_{21}(j\Omega)|^2} \text{dB}$$

1.1.1 Poles and Zeros of Complex Plane:

The (σ,Ω) plane, where a rational transfer function is defined, is called the complex plane or the p-plane. The horizontal axis of this plane is called the real or σ-axis, and the vertical axis is called the imaginary or jΩ-axis. The value of p at which the function becomes zero are the zeroes of the function, and the values of at which the the function becomes infinite are singularities (usually the poles) of the function. Therefore, the zeroes of $S_{21}(p)$ are the roots of the numerator N(p) and the poles are the roots of denominator D(p).

These poles will be the natural frequencies of the filter whose response is described by $S_{21}(p)$. For the filter to be stable, these frequencies must lie in the left half of the p-plane, or on the imaginary axis. If this were not so, the oscillations would be of exponentially increasing magnitude with respect to time, which is impossible in any passive network.

The poles and zeros of a rational transfer function may be depicted on the p-plane. Based on their locations there are different types of transfer functions which we are going to discuss now.

1.1.2 Butterworth (Maximally Flat) Response:

The amplitude-squared transfer function for Butterworth filters that have an insertion loss L_{Ar} = 3.01 dB at the cutoff frequency $\Omega_c = 1$ is given by

$$|S_{21}(j\Omega)|^2 = \frac{1}{1+\Omega^{2n}}$$

Where n is the degree or the order of filter, which corresponds to the number of reactive elements required in the low pass prototype filter. This type response is also referred to as maximally flat because its amplitude-squared transfer function defined above have the maximum number of (2n-1) zero derivatives at Ω=0. Therefore. The maximally flat approximation to the ideal lowpass filter in the passband is best at Ω=0, but deteriorates as Ω approaches the cutoff frequency Ω_c.

A rational transfer function can be constructed from the above amplitude-squared function:

$$S_{21}(p) = \frac{1}{\prod_{i=1}^{n}(p-p_i)}$$

with

$$p_i = j\exp\left[\frac{(2i-1)\pi}{2n}\right]$$

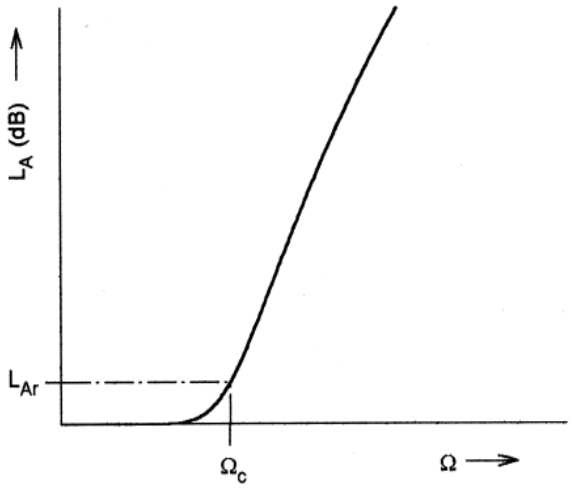

Figure 1.1 Butterworth Filter Response

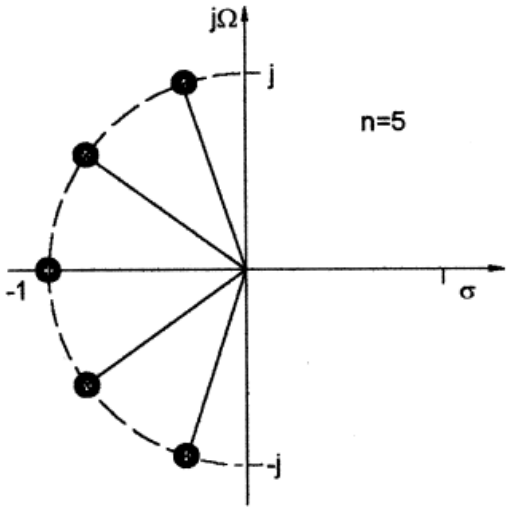

Figure 2.2 Pole Locations for Butterworth Filter Response

1.1.3 Chebyshev Response:

The Chebyshev response that exhibits the equal-ripple passband and maximally flat stopband is shown below. The amplitude-squared transfer function that describes this type of response is

$$|S_{21}(j\Omega)|^2 = \frac{1}{1 + \varepsilon^2 T_n^2(\Omega)}$$

where the ripple constant ε is related to a given passband ripple L_{Ar} in dB by

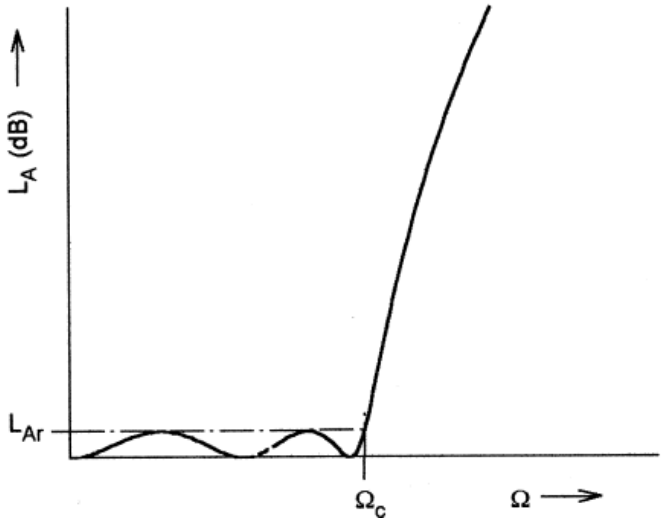

Figure 1.3 Chebyshev Filter Response

$T_n(\Omega)$ is a Chebyshev function of the first kind of order n, which is defined as

$$T_n(\Omega) = \begin{cases} \cos(n \cos^{-1} \Omega) & |\Omega| \leq 1 \\ \cosh(n \cosh^{-1} \Omega) & |\Omega| \geq 1 \end{cases}$$

Hence, the filters realized from these equations are commonly known as Chebyshev filters. General formula of the rational transfer function for the Chebyshev filter is given by

$$S_{21}(p) = \frac{\prod_{i=1}^{n} [\eta^2 + \sin^2(i\pi/n)]^{1/2}}{\prod_{i=1}^{n} (p + p_i)}$$

with

$$p_i = j \cos\left[\sin^{-1} j\eta + \frac{(2i-1)\pi}{2n} \right]$$

$$\eta = \sinh\left(\frac{1}{n} \sinh^{-1} \frac{1}{\varepsilon} \right)$$

Like the maximally flat case, all the transmission zeros of $S_{21}(p)$ are located at infinity. Therefore, the Butterworth and Chebyshev filters dealt with so far are sometimes referred to as all-pole filters. However, the pole locations for the Chebyshev case are different, and lie on an ellipse in the left half-plane. The major axis of the ellipse is on the jΩ-axis and its size is $\sqrt{1+\eta^2}$; the minor axis is on the σ-axis and is of the size η. The pole distribution is shown, for n=5.

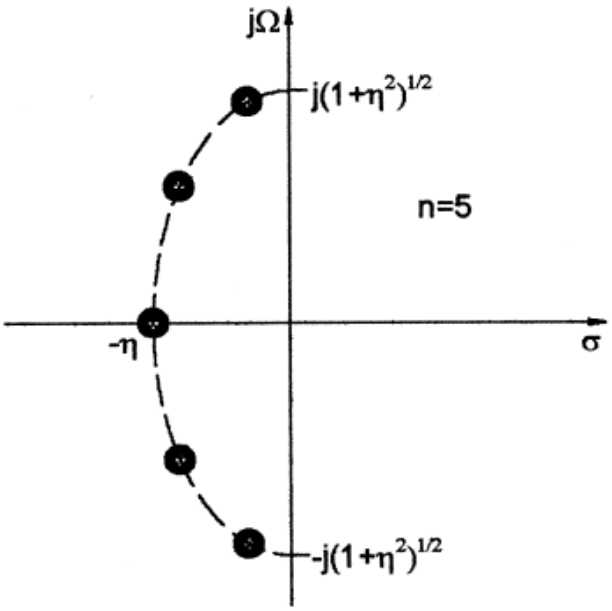

Figure 1.4 Pole Location for Chebyshev Filter Response

1.1.4 Elliptic Function Response:

The response that is equal-ripple in both the passband and stopband is the elliptic function response. The transfer function for this type of response is

$$|S_{21}(j\Omega)|^2 = \frac{1}{1 + \varepsilon^2 F_n^2(\Omega)}$$

with

$$F_n(\Omega) = \begin{cases} M \dfrac{\prod_{i=1}^{n/2}(\Omega_i^2 - \Omega^2)}{\prod_{i=1}^{n/2}(\Omega_s^2/\Omega_i^2 - \Omega^2)} & \text{for } n \text{ even} \\ N \dfrac{\Omega \prod_{i=1}^{(n-1)/2}(\Omega_i^2 - \Omega^2)}{\prod_{i=1}^{(n-1)/2}(\Omega_s^2/\Omega_i^2 - \Omega^2)} & \text{for } n(\geq 3) \text{ odd} \end{cases}$$

Where Ω_i ($0 < \Omega_i < 1$) and $\Omega_s > 1$ represents some critical frequencies; M and N are constants.

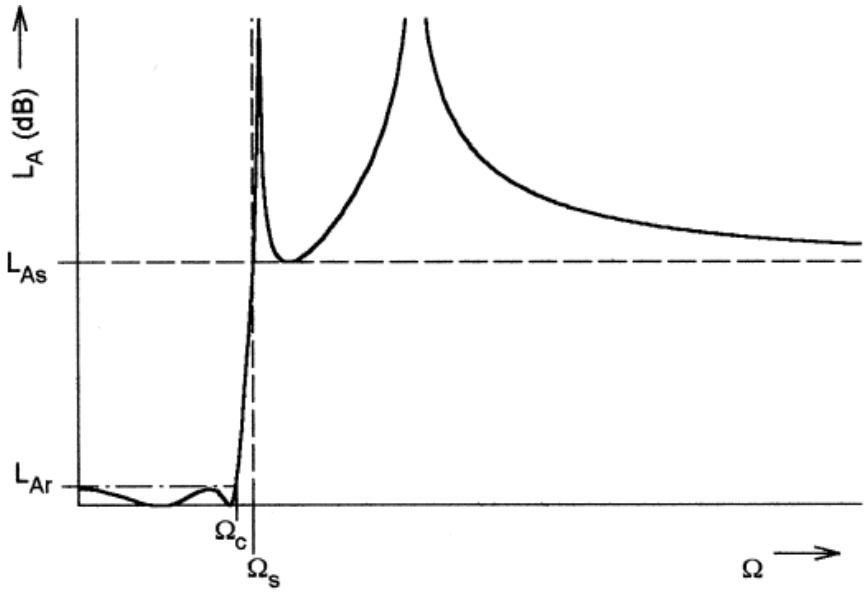

Figure 1.5 Elliptic Filter Response

1.1.5 Gaussian (Maximally Flat Group-Delay) Response:

The Gaussian response is approximated by a rational transfer function

$$S_{21}(p) = \frac{a_0}{\sum_{k=0}^{n} a_k p^k}$$

Where $p = \sigma + j\Omega$ is the normalized complex frequency variable, and the coefficients

$$a_k = \frac{(2n-k)!}{2^{n-k} k!(n-k)!}$$

This transfer function possesses a group delay that has maximum possible number of zero derivatives with respect to Ω at Ω = 0, which is why it is said to have maximally flat group delay around Ω = 0 and is in a sense complementary to the Butterworth response, which has a maximally flat amplitude. The filters of this type are also known as Bessel filters.

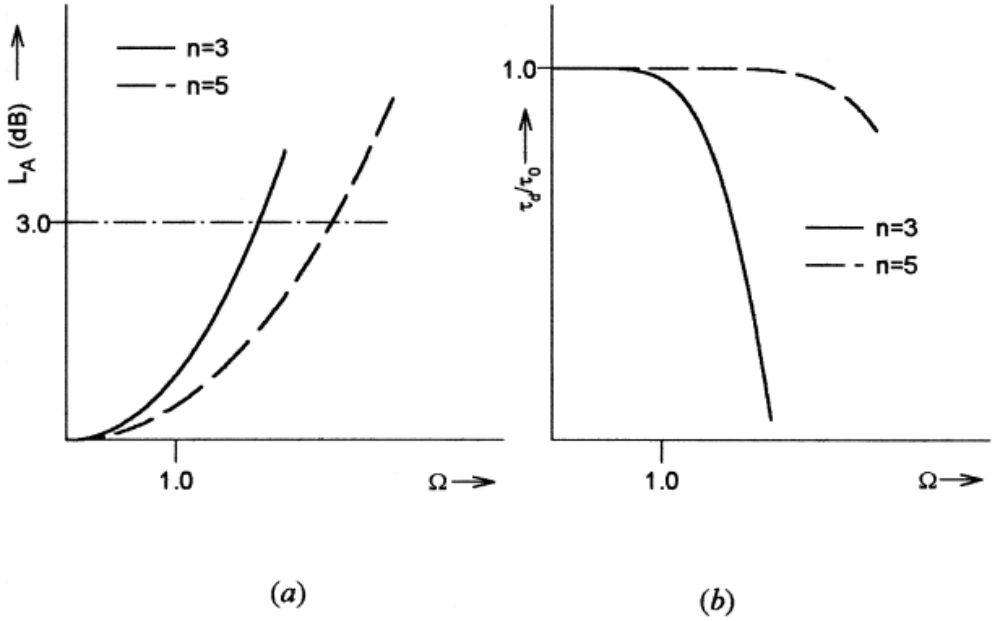

Figure 1.6 Gaussian Filter Response (a) Amplitude (b) Phase Delay

1.2 Low pass Prototype Filters and Elements

Filter syntheses for realizing the transfer functions that are discussed above, usually result in the so-called low pass prototype filters. A low pass prototype filter is in general defined as the low pass filter whose element values are normalized to make the source resistance or conductance equal to one denoted by $g_0 = 1$, and the cut-off angular frequency to be unity, denoted by Ωc = 1(rad/s). This type of low pass filter can serve as a prototype for designing many practical filters with frequency and element transformations. This will be addressed in the next section. Below are the prototype filters for different type of filter responses.

1.2.1 Butterworth Low pass Prototype Filters

For Butterworth or maximally flat low pass prototype filters having a transfer function given above with an insertion loss L_{Ar} = 3.01 dB at the cut-off Ωc = 1, the element values may be computed by

$$g_0 = 1.0$$

$$g_i = 2 \sin\left(\frac{(2i-1)\pi}{2n}\right) \qquad \text{for } i = 1 \text{ to } n$$

$$g_{n+1} = 1.0$$

As can be seen, the two-port Butterworth filters considered here are always symmetrical in network structure, namely, $g_0 = g_{n+1}$, $g_1 = g_n$ and so on.

To determine the degree of a Butterworth low pass prototype, a specification that is usually the minimum stopband attenuation L_{As} dB at $\Omega = \Omega s$ for $\Omega s > 1$ is given. Hence

$$n \geq \frac{\log(10^{0.1L_{AS}} - 1)}{2\log\Omega_s}$$

1.2.2 Chebyshev Low pass Prototype Filters

For Chebyshev low pass prototype filters having a transfer function given earlier with a passband ripple L_{Ar} dB and the cutoff frequency $\Omega c = 1$, the element values for the two-port networks may be computed using the following formulas:

$$g_0 = 1.0$$

$$g_1 = \frac{2}{\gamma}\sin\left(\frac{\pi}{2n}\right)$$

$$g_i = \frac{1}{g_{i-1}} \frac{4\sin\left[\frac{(2i-1)\pi}{2n}\right]\cdot\sin\left[\frac{(2i-3)\pi}{2n}\right]}{\gamma^2 + \sin^2\left[\frac{(i-1)\pi}{n}\right]} \qquad \text{for } i = 2, 3, \cdots n$$

$$g_{n+1} = \begin{cases} 1.0 & \text{for } n \text{ odd} \\ \coth^2\left(\frac{\beta}{4}\right) & \text{for } n \text{ even} \end{cases}$$

where

$$\beta = \ln\left[\coth\left(\frac{L_{Ar}}{17.37}\right)\right]$$

$$\gamma = \sinh\left(\frac{\beta}{2n}\right)$$

For the required passband ripple L_{Ar} dB, the minimum stopband attenuation L_{As} dB at $\Omega = \Omega s$, the degree of a Chebyshev low pass prototype, which will meet this specification, can be found by

$$n \geq \frac{\cosh^{-1}\sqrt{\dfrac{10^{0.1L_{As}}-1}{10^{0.1L_{Ar}}-1}}}{\cosh^{-1}\Omega_s}$$

Sometimes, the minimum return loss L_R or the maximum voltage standing wave ratio VSWR in the passband is specified instead of the passband ripple L_{Ar}. If the return loss is defined and the minimum passband return loss is L_R dB ($L_R < 0$), the corresponding passband ripple is

$$L_{Ar} = -10\log(1 - 10^{0.1L_R})\ \text{dB}$$

1.2.3 Elliptic Function Low pass Prototype Filters

Figure 1.7 illustrates two commonly used network structures for elliptic function low pass prototype filters. In Figure 1.7(a), the series branches of parallel-resonant circuits are introduced for realizing the finite-frequency transmission zeros, since they block transmission by having infinite series impedance (open-circuit) at resonance. For this form of the elliptic function low pass prototype [Figure 1.7(a)], g_i for odd i(i = 1, 3, · · ·) represent the capacitance of a shunt capacitor, g_i for even i (i = 2, 4, · · ·) represent the inductance of an inductor, and the primed g'_i for even i (i = 2, 4, · · ·) are the capacitance of a capacitor in a series branch of parallel-resonant circuit. For the dual realization form in Figure 1.7(b), the shunt branches of series-resonant circuits are used for implementing the finite-frequency transmission zeros, since they short out transmission at resonance. In this case, referring to Figure 1.7(b), g_i for odd i (i = 1, 3, · · ·) are the inductance of a series inductor, g_i for even i (i = 2, 4, · · ·) are the capacitance of a capacitor, and primed g'_i for even i(i = 2, 4, · · ·) indicate the inductance of an inductor in a shunt branch of series-resonant circuit. Again, either form may be used, because both give the same response.

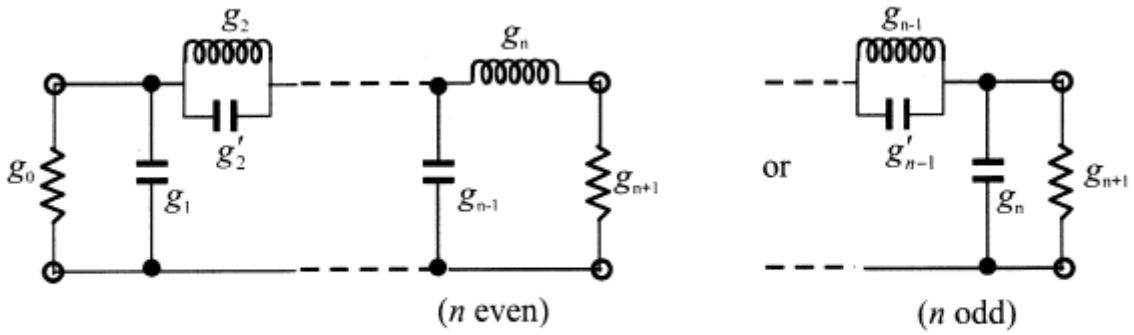

(a)

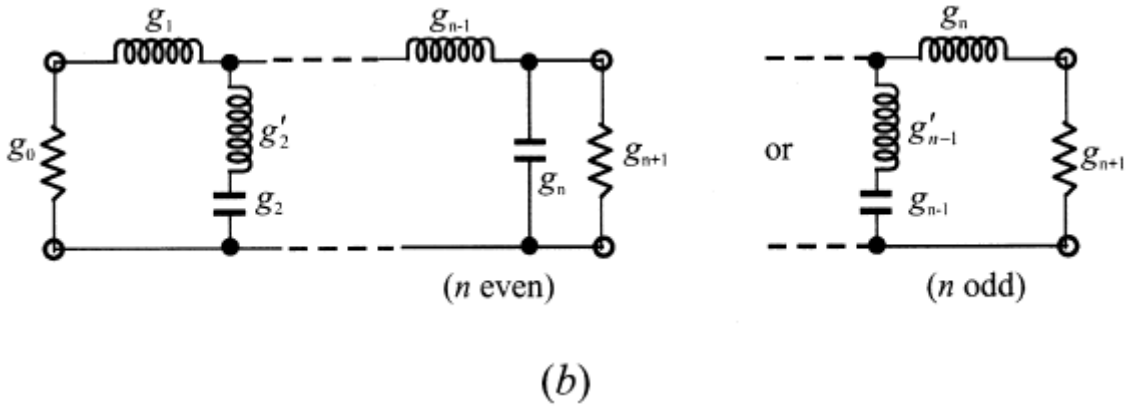

(b)

Figure 1.7 Lowpass prototype filters for elliptic function filters with (a) series parallel-resonant

Unlike the Butterworth and Chebyshev low pass prototype filters, there is no simple formula available for determining element values of the elliptic function low pass prototype filters.

1.3 Frequency and Element Transformations

So far, we have only considered the low pass prototype filters, which have a normalized source resistance/conductance $g_0 = 1$ and a cut-off frequency $\Omega c = 1$. To obtain frequency characteristics and element values for practical filters based on the low pass prototype, one may apply frequency and element transformations, which will be addressed in this section.

The frequency transformation, which is also referred to as frequency mapping, is required to map a response such as Chebyshev response in the low pass prototype frequency domain ω to that in the frequency domain Ω in which a practical filter response such as low pass, high pass, band pass, and band stop are expressed. The frequency transformation will influence all the reactive elements accordingly, but no effect on the resistive elements. In addition to the frequency mapping, impedance scaling is also required to accomplish the element transformation. The impedance scaling will remove the $g_0 = 1$ normalization and adjust the filter to work for any value of the source impedance denoted by Z_0. For our formulation, it is convenient to define an impedance scaling factor γ_0 as

$$\gamma_0 = \begin{cases} Z_0/g_0 & \text{for } g_0 \text{ being the resistance} \\ g_0/Y_0 & \text{for } g_0 \text{ being the conductance} \end{cases}$$

where $Y_0 = 1/Z_0$ is the source admittance. In principle, applying the impedance scaling upon a filter network in such a way that has no effect on the response shape.

$$L \rightarrow \gamma_0 L \qquad R \rightarrow \gamma_0 R$$
$$C \rightarrow C/\gamma_0 \qquad G \rightarrow G/\gamma_0$$

Let g be the generic term for the low pass prototype elements in the element transformation to be discussed. Because it is independent of the frequency transformation, the following resistive element transformation holds for any type of filter:

$$R = \gamma_0 g \quad \text{for } g \text{ representing the resistance}$$

$$G = \frac{g}{\gamma_0} \quad \text{for } g \text{ representing the conductance}$$

1.3.1 Low pass Transformation

The frequency transformation from a low pass prototype to a practical low pass filter having a cut-off frequency ω_c in the angular frequency axis ω is simply given by

$$\Omega = \left(\frac{\Omega_c}{\omega_c}\right)\omega$$

Applying the above formula together with the impedance scaling described earlier yields the element transformation:

$$L = \left(\frac{\Omega_c}{\omega_c}\right)\gamma_0 g \quad \text{for } g \text{ representing the inductance}$$

$$C = \left(\frac{\Omega_c}{\omega_c}\right)\frac{g}{\gamma_0} \quad \text{for } g \text{ representing the capacitance}$$

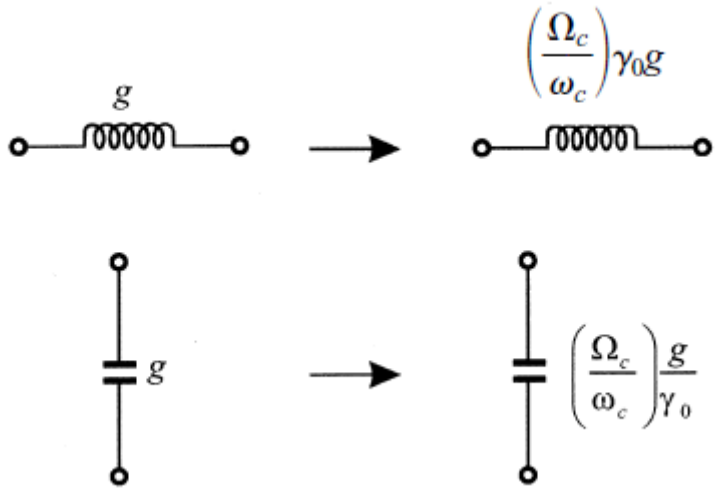

Figure 1.8 Lowpass prototype to lowpass transformation for basic elements

1.3.2 High pass Transformation

For high pass filters with a cut-off frequency ω_c in the ω-axis, the frequency transformation is

$$\Omega = -\frac{\omega_c \Omega_c}{\omega}$$

Applying this frequency transformation to a reactive element g in the low pass prototype leads to

$$j\Omega g \rightarrow \frac{\omega_c \Omega_c g}{j\omega}$$

It is then obvious that an inductive/capacitive element in the low pass prototype will be inversely transformed to a capacitive/inductive element in the high pass filter. With impedance scaling, the element transformation is given by

$$C = \left(\frac{1}{\omega_c \Omega_c}\right)\frac{1}{\gamma_0 g} \quad \text{for } g \text{ representing the inductance}$$

$$L = \left(\frac{1}{\omega_c \Omega_c}\right)\frac{\gamma_0}{g} \quad \text{for } g \text{ representing the capacitance}$$

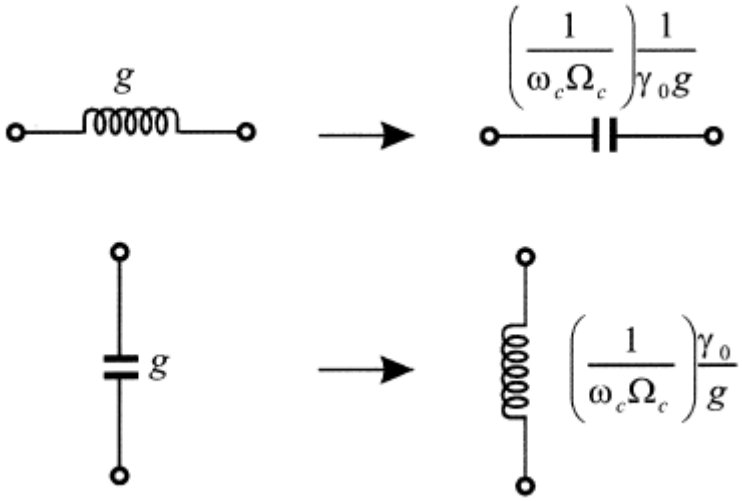

Figure 1.9 Low pass prototype to high pass transformation for basic element transformation

1.3.3 Band pass Transformation

Assume that a low pass prototype response is to be transformed to a band pass response having a passband $\omega_2 - \omega_1$, where ω_1 and ω_2 indicate the passband-edge angular frequency. The required frequency transformation is

$$\Omega = \frac{\Omega_c}{FBW}\left(\frac{\omega}{\omega_0} - \frac{\omega_0}{\omega}\right)$$

with

$$FBW = \frac{\omega_2 - \omega_1}{\omega_0}$$

$$\omega_0 = \sqrt{\omega_1 \omega_2}$$

where ω_0 denotes the center angular frequency and FBW is defined as the fractional bandwidth. If we apply this frequency transformation to a reactive element g of the low pass prototype, we have

$$j\Omega g \rightarrow j\omega \frac{\Omega_c g}{FBW\omega_0} + \frac{1}{j\omega}\frac{\Omega_c \omega_0 g}{FBW}$$

which implies that an inductive/capacitive element g in the low pass prototype will transform to a series/parallel LC resonant circuit in the band pass filter. The elements for the series LC resonator in the band pass filter are

$$L_s = \left(\frac{\Omega_c}{FBW\omega_0}\right)\gamma_0 g$$

$$C_s = \left(\frac{FBW}{\omega_0 \Omega_c}\right)\frac{1}{\gamma_0 g}$$

for g representing the inductance

Where the impedance scaling has been considered as well. Similarly, the elements for the parallel LC resonator in the band pass filter are

$$C_p = \left(\frac{\Omega_c}{FBW\omega_0}\right)\frac{g}{\gamma_0}$$

$$L_p = \left(\frac{FBW}{\omega_0 \Omega_c}\right)\frac{\gamma_0}{g}$$

for g representing the capacitance

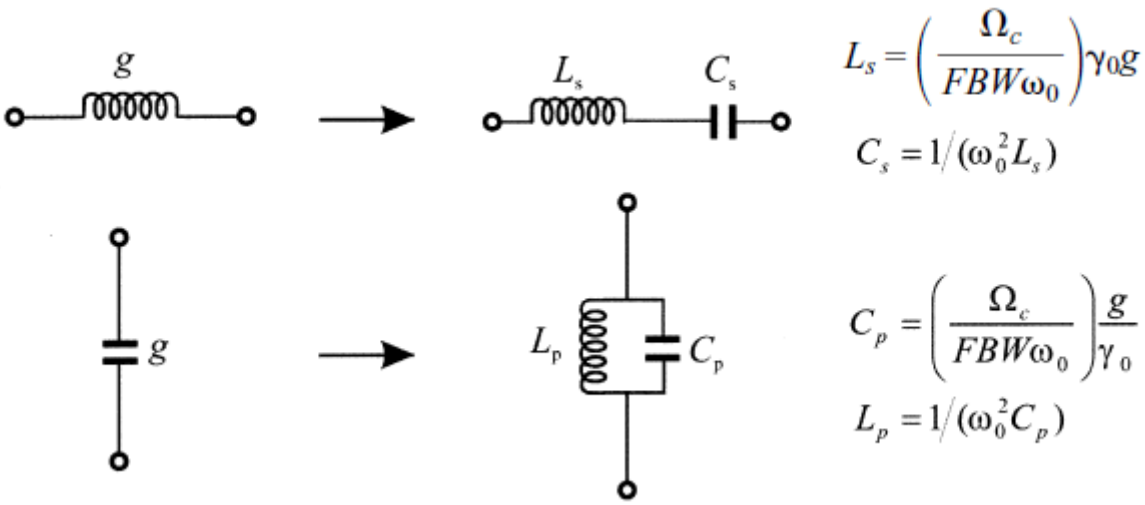

Figure 1.10 Lowpass prototype to bandpass transformation for basic element transformation

1.3.4 Band stop Transformation

The frequency transformation from low pass prototype to band strop is achieved by the frequency mapping

$$\Omega = \frac{\Omega_c FBW}{(\omega_0/\omega - \omega/\omega_0)}$$

$$\omega_0 = \sqrt{\omega_1 \omega_2}$$

$$FBW = \frac{\omega_2 - \omega_1}{\omega_0}$$

where $\omega_2 - \omega_1$ is the bandwidth. This form of the transformation is opposite to the band pass transformation in that an inductive/capacitive element g in the low pass prototype will transform to a parallel/series LC resonant circuit in the band stop filter. The elements for the LC resonators transformed to the band stop filter are

$$C_p = \left(\frac{1}{FBW\omega_0\Omega_c}\right)\frac{1}{\gamma_0 g}$$

for g representing the inductance

$$L_p = \left(\frac{\Omega_c FBW}{\omega_0}\right)\gamma_0 g$$

$$L_s = \left(\frac{1}{FBW\omega_0\Omega_c}\right)\frac{\gamma_0}{g}$$

for g representing the capacitance

$$C_s = \left(\frac{\Omega_c FBW}{\omega_0}\right)\frac{g}{\gamma_0}$$

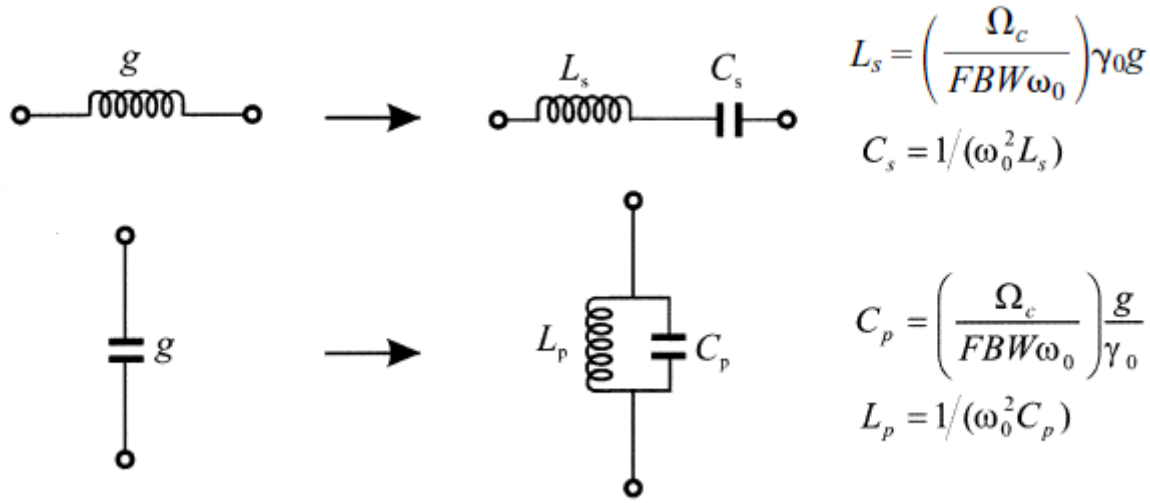

Figure 1.11 Lowpass prototype to bandpass transformation for basic element transformation

1.4 Filter Design by The Insertion Loss Method

A perfect filter would have zero insertion loss in the passband, infinite attenuation in the stopband, and a linear phase response (to avoid signal distortion) in the passband. Of course, such filters do not exist in practice, so compromises must be made; herein lies the art of filter design. The image parameter method of the previous section may yield a usable filter response for some applications, but there is no methodical way of improving the design. The insertion loss method, however, allows a high degree of control over the passband and stopband amplitude and phase characteristics, with a systematic way to synthesize a desired response. The necessary design trade-offs can be evaluated to best meet the application requirements. If, for example, a minimum insertion loss is most important, a binomial response could be used; a Chebyshev response would satisfy a requirement for the sharpest cut-off. If it is possible to sacrifice the attenuation rate, a better phase response can be obtained by using a linear phase filter design. In addition, in all cases, the insertion loss method allows filter performance to be improved in a straightforward manner, at the expense of a higher order filter. For the filter prototypes to be discussed below, the order of the filter is equal to the number of reactive elements.

Characterisation by Power Loss Ratio:

In the insertion loss method, a filter response is defined by its insertion loss, or *power loss ratio, P_{LR}:*

$$P_{\mathrm{LR}} = \frac{\text{Power available from source}}{\text{Power delivered to load}} = \frac{P_{\mathrm{inc}}}{P_{\mathrm{load}}} = \frac{1}{1 - |\Gamma(\omega)|^2}.$$

Observe that this quantity is the reciprocal of $|S_{21}|^2$ if both load and source are matched. The insertion loss (IL) in dB is given by:

$$\mathrm{IL} = 10 \log P_{\mathrm{LR}}$$

1.5 Filter Implementation

The lumped-element filter designs discussed in the previous sections generally work well at low frequencies, but two problems arise at higher RF and microwave frequencies. First, lumped-element inductors and capacitors are generally available only for a limited range of values, and can be difficult to implement at microwave frequencies. Distributed elements, such as open-circuited or short-circuited transmission line stubs, are often used to approximate ideal lumped elements. In addition, at microwave frequencies the distances between filter components is not negligible. The first problem is treated with Richards' transformation, which can be used to convert lumped elements to transmission line sections. Kuroda's identities can then be used to physically separate filter elements by using transmission line sections. Because such additional transmission line sections do not affect the filter response, this type of design is called redundant filter synthesis. It is possible to design microwave filters that take advantage of these sections to improve the filter response; such no redundant synthesis does not have a lumped-element counterpart.

1.5.1 Richards' Transformation

The transformation

$$\Omega = \tan\beta\ell = \tan\left(\frac{\omega\ell}{v_p}\right)$$

maps the ω plane to the plane, which repeats with a period of $\omega l / v_p = 2\pi$. This transformation was introduced by P. Richards to synthesize an LC network using open- and short-circuited transmission line stubs. Thus, if we replace the frequency variable ω with, we can write the reactance of an inductor as

$$jX_L = j\Omega L = jL\tan\beta\ell,$$

and the susceptance of a capacitor as

$$jB_C = j\Omega C = jC\tan\beta\ell$$

These results indicate that an inductor can be replaced with a short-circuited stub of length β and characteristic impedance L, while a capacitor can be replaced with an open-circuited stub of length β and characteristic impedance 1/C. A unity filter impedance is assumed. Cutoff occurs at unity frequency for a low-pass filter prototype; to obtain the same cutoff frequency for the Richards'-transformation filter, shows that

$$\Omega = 1 = \tan\beta\ell,$$

which gives a stub length of = λ/8, where λ is the wavelength of the line at the cutoff frequency, ω_c. At the frequency $\omega_0 = 2\omega_c$, the lines will be λ/4 long, and an attenuation pole will occur. At frequencies away from ω_c, the impedances of the stubs will no longer match the original lumped-element impedances, and the filter response will differ from the desired prototype response. In addition, the response will be periodic in frequency, repeating every $4\omega_c$. In principle, then, Richards' transformation allows the inductors and capacitors of a lumped-

element filter to be replaced with short-circuited and open-circuited transmission line stubs, as illustrated in Figure 1.12. Since the electrical lengths of all the stubs are the same (λ/8 at ω_c), these lines are called commensurate lines.

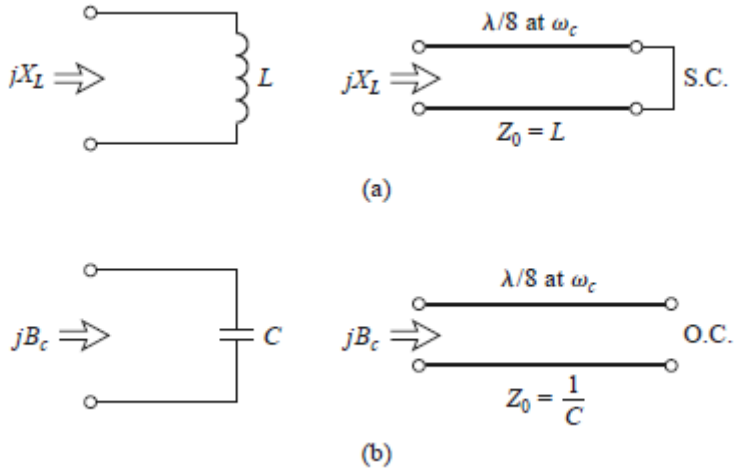

Figure 1.12 Richards' Transformation (a) For inductor to a short-circuited stub (b) For a capacitor to an open-circuited stub

1.5.2 Kuroda's Identities

The four Kuroda identities use redundant transmission line sections to achieve a more practical microwave filter implementation by performing any of the following operations:

- Physically separate transmission line stubs
- Transform series stubs into shunt stubs, or vice versa
- Change impractical characteristic impedance into more realizable values

The additional transmission line sections are called unit elements and are λ/8 long at ω_c; the unit elements are thus commensurate with the stubs used to implement the inductors and capacitors of the prototype design. The four Kuroda identities are illustrated in the following table, where each box represents a unit element, or transmission line, of the indicated characteristic impedance and length (λ/8 at ω_c). The inductors and capacitors represent short-circuit and open-circuit stubs, respectively.

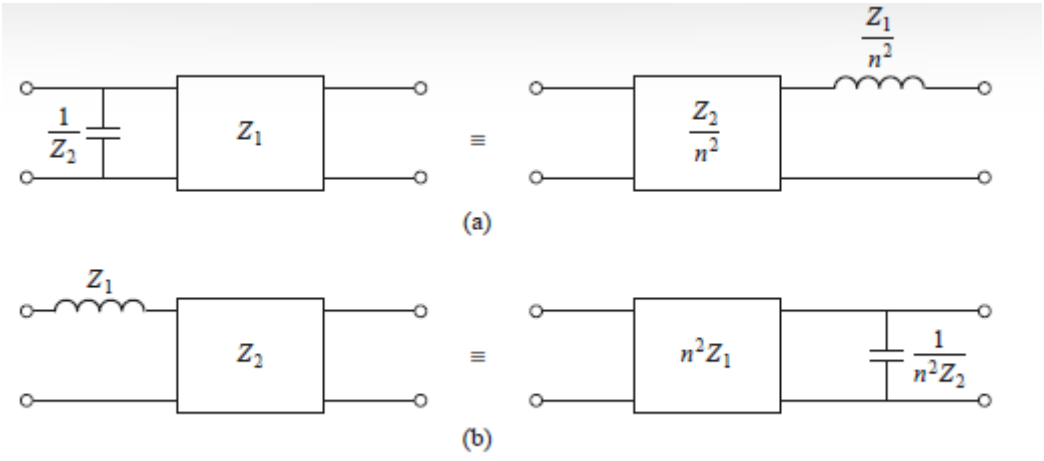

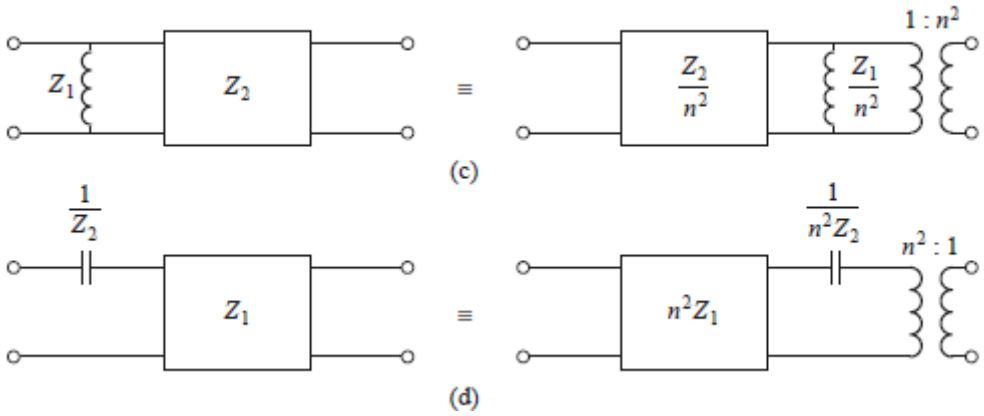

Figure 1.13 The four Kuroda Identities

The following graph shows the response of a low-pass filter response with a cut-off at 4Ghz and impedance of 50 Ω, designed using both lumped and distributed elements.

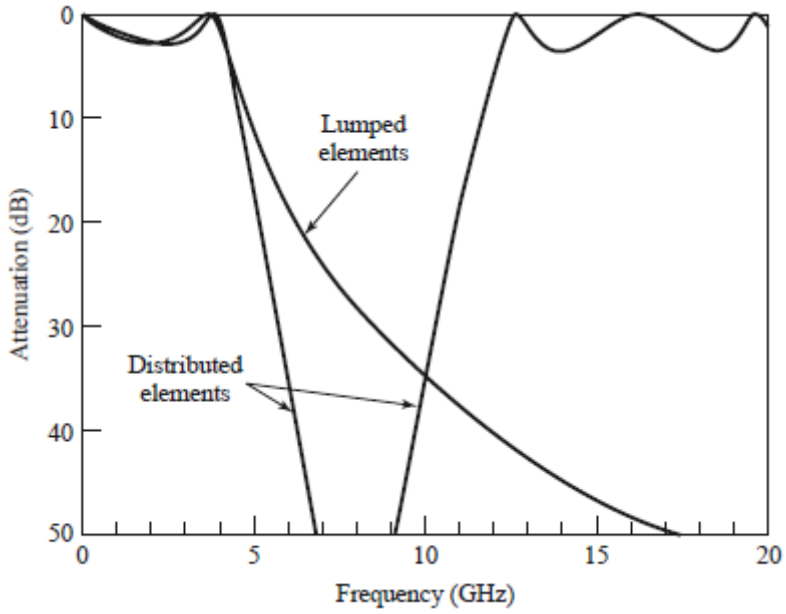

Figure 1.14 Filter Response for both lumped and distributed elements

As we can see, even though the passband characteristics are very similar up to 4Ghz, but the distributed-element filter has a sharper cutoff. Also, the response of distributed-element filter repeats every 16Ghz, because of the periodicity of Richards' transformation.

1.5.3 Impedance and Admittance Inverters

As we have seen, it is often desirable to use only series, or only shunt, elements when implementing a filter with a particular type of transmission line. The Kuroda identities can be used for conversions of this form, but another possibility is to use impedance (K) or admittance (J) inverters. Such inverters are especially useful for bandpass or bandstop filters with narrow (<10%) bandwidths. The conceptual operation of impedance and admittance inverters is illustrated in Figure 8.38; since these inverters essentially form the inverse of the load impedance or admittance, they can be used to transform series-connected elements to shunt-connected elements, or vice versa.

CHAPTER-2: TRANSMISSION LINES AND COMPONENTS

In this chapter, basic concepts, and design equations for micro strip lines, coupled micro strip lines, discontinuities, and components useful for design of filters are briefly described.

2.1 *Micro strip Lines*

2.1.1 Micro strip Structure

The general structure of a micro strip is illustrated in Figure 2.1. A conducting strip (micro strip line) with a width W and a thickness t is on the top of a dielectric substrate that has a relative dielectric constant ε_r and a thickness h, and the bottom of the substrate is a ground (conducting) plane.

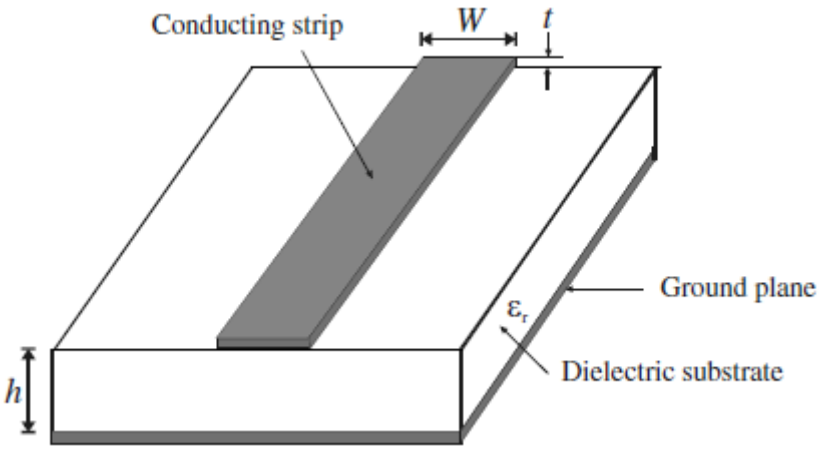

Figure 3.1 General Microstrip Structure

2.1.2 Waves in Micro strips

The fields in the micro strip extend within two media—air above and dielectric below— so that the structure is inhomogeneous. Due to this inhomogeneous nature, the micro strip does not support a pure TEM wave. This is because that a pure TEM wave has only transverse components, and its propagation velocity depends only on the material properties, namely the permittivity ε and the permeability μ. However, with the presence of the two guided-wave media (the dielectric substrate and the air), the waves in a micro strip line will have no vanished longitudinal components of electric and magnetic fields, and their propagation velocities will depend not only on the material properties, but also on the physical dimensions of the micro strip.

2.1.3 Quasi-TEM Approximation

When the longitudinal components of the fields for the dominant mode of a micro strip line remain very much smaller than the transverse components, they may be neglected. In this case, the dominant mode then behaves like a TEM mode, and the TEM transmission line theory is

applicable for the micro strip line as well. This is called the quasi-TEM approximation and it is valid over most of the operating frequency ranges of micro strip.

2.1.4 Effective Dielectric Constant and Characteristic Impedance

In the quasi-TEM approximation, a homogeneous dielectric material with an effective dielectric permittivity replaces the inhomogeneous dielectric–air media of micro strip. Transmission characteristics of micro strips are described by two parameters, namely, the effective dielectric constant ε_{re} and characteristic impedance Z_c, which may then be obtained by quasistatic analysis [1]. In quasi-static analysis, the fundamental mode of wave propagation in a micro strip is assumed to be pure TEM. The above two parameters of micro strips are then determined from the values of two capacitances as follows

$$\varepsilon_{re} = \frac{C_d}{C_a}$$

$$Z_c = \frac{1}{c\sqrt{C_a C_d}}$$

in which C_d is the capacitance per unit length with the dielectric substrate present, C_a is the capacitance per unit length with the dielectric substrate replaced by air, and c is the velocity of electromagnetic waves in free space ($c = 3.0 \times 10^8$ m/s). For very thin conductors (i.e., t->0), the closed-form expressions that provide an accuracy better than 1% are given as follows:

$$\varepsilon_{re} = \frac{\varepsilon_r + 1}{2} + \frac{\varepsilon_r - 1}{2}\left\{\left(1 + 12\frac{h}{W}\right)^{-0.5} + 0.04\left(1 - \frac{W}{h}\right)^2\right\}$$

$$Z_c = \frac{\eta}{2\pi\sqrt{\varepsilon_{re}}} \ln\left(\frac{8h}{W} + 0.25\frac{W}{h}\right)$$

where $\eta = 120\pi$ ohms is the wave impedance in free space.

For W/h >= 1:

$$\varepsilon_{re} = \frac{\varepsilon_r + 1}{2} + \frac{\varepsilon_r - 1}{2}\left(1 + 12\frac{h}{W}\right)^{-0.5}$$

$$Z_c = \frac{\eta}{\sqrt{\varepsilon_{re}}}\left\{\frac{W}{h} + 1.393 + 0.677 \ln\left(\frac{W}{h} + 1.444\right)\right\}^{-1}$$

2.1.5 Guided Wavelength, Propagation Constant, Phase Velocity, and Electrical Length

Once the effective dielectric constant of a microstrip is determined, the guided wavelength of the quasi-TEM mode of microstrip is given by

$$\lambda_g = \frac{\lambda_0}{\sqrt{\varepsilon_{re}}}$$

where λ_0 is the free space wavelength at operation frequency f. More conveniently, where the frequency is given in gigahertz (GHz), the guided wavelength can be evaluated directly in millimetres as follows:

$$\lambda_g = \frac{300}{f(\text{GHz})\sqrt{\varepsilon_{re}}} \text{ mm}$$

The associated propagation constant β and phase velocity v_p can be determined by

$$\beta = \frac{2\pi}{\lambda_g}$$

$$v_p = \frac{\omega}{\beta} = \frac{c}{\sqrt{\varepsilon_{re}}}$$

where c is the velocity of light in free space. The electrical length θ for a given physical length l of the microstrip is defined by

$$\theta = \beta l$$

Therefore = π/2 when $l = \lambda_g/4$, and θ = π when $l = \lambda_g/2$. These so-called quarter wavelength and half-wavelength micro strip lines are important for design of micro strip filters.

2.1.6 Synthesis of W/h

Approximate expressions for W/h in terms of Z_c and ε_r are given as follows:

For $W/h \leq 2$

$$\frac{W}{h} = \frac{8\exp(A)}{\exp(2A) - 2}$$

with

$$A = \frac{Z_c}{60}\left\{\frac{\varepsilon_r + 1}{2}\right\}^{0.5} + \frac{\varepsilon_r - 1}{\varepsilon_r + 1}\left\{0.23 + \frac{0.11}{\varepsilon_r}\right\}$$

and for $W/h \geq 2$

$$\frac{W}{h} = \frac{2}{\pi}\left\{(B-1) - \ln(2B-1) + \frac{\varepsilon_r - 1}{2\varepsilon_r}\left[\ln(B-1) + 0.39 - \frac{0.61}{\varepsilon_r}\right]\right\}$$

with

$$B = \frac{60\pi^2}{Z_c\sqrt{\varepsilon_r}}$$

These expressions also provide accuracy better than 1%. If more accurate values are needed, an iterative or optimization process based on the more accurate analysis models can be employed.

2.1.7 Effect of Strip Thickness

So far, we have not considered the effect of conducting strip thickness t (as referring to Figure 2.1). The thickness t is usually very small when the micro strip line is realized by conducting thin films; therefore, its effect may quite often be neglected. Nevertheless, its effect on the characteristic impedance and effective dielectric constant may be included

For $W/h \leq 1$:

$$Z_c(t) = \frac{\eta}{2\pi\sqrt{\varepsilon_{re}}} \ln\left\{ \frac{8}{W_e(t)/h} + 0.25\frac{W_e(t)}{h} \right\}$$

For $W/h \geq 1$:

$$Z_c(t) = \frac{\eta}{\sqrt{\varepsilon_{re}}} \left\{ \frac{W_e(t)}{h} + 1.393 + 0.667 \ln\left(\frac{W_e(t)}{h} + 1.444 \right) \right\}^{-}$$

where

$$\frac{W_e(t)}{h} = \begin{cases} \frac{W}{h} + \frac{1.25}{\pi}\frac{t}{h}\left(1 + \ln\frac{4\pi W}{t}\right) & (W/h \leq 0.5\pi) \\ \frac{W}{h} + \frac{1.25}{\pi}\frac{t}{h}\left(1 + \ln\frac{2h}{t}\right) & (W/h \geq 0.5\pi) \end{cases}$$

$$\varepsilon_{re}(t) = \varepsilon_{re} - \frac{\varepsilon_r - 1}{4.6}\frac{t/h}{\sqrt{W/h}}$$

In the above expressions, ε_{re} is the effective dielectric constant for t = 0. It can be observed that the effect of strip thickness on both the characteristic impedance and effective dielectric constant is insignificant for small values of t/h. However, the effect of strip thickness is significant for conductor loss of the micro strip line.

2.2 Microstrip Discontinuities

Microstrip discontinuities commonly encountered in the layout of practical filters include steps, open-ends, bends, gaps, and junctions. Figure 4.4 illustrates some typical structures and their equivalent circuits. The effects of discontinuities can be more accurately modelled and considered in the filter designs with full-wave electromagnetic (EM) simulations, which will be addressed in due course later. Nevertheless, closed-form expressions for equivalent circuit models of these discontinuities are still useful whenever they are appropriate. These expressions are used in many circuit analysis programs. There are numerous closed form

expressions for microstrip discontinuities available, for convenience some typical ones are given as follows.

2.2.1 Steps in Width

For a symmetrical step, the capacitance and inductances of the equivalent circuit indicated below may approximated by the following formulation

$$C = 0.00137h\,\frac{\sqrt{\varepsilon_{re1}}}{Z_{c1}}\left(1-\frac{W_2}{W_1}\right)\left(\frac{\varepsilon_{re1}+0.3}{\varepsilon_{re1}-0.258}\right)\left(\frac{W_1/h+0.264}{W_1/h+0.8}\right)\text{(pF)}$$

$$L_1 = \frac{L_{w1}}{L_{w1}+L_{w2}}L, \quad L_2 = \frac{L_{w2}}{L_{w1}+L_{w2}}L$$

with

$$L_{wi} = Z_{ci}\sqrt{\varepsilon_{rei}}/c$$

$$L = 0.000987h\left(1-\frac{Z_{c1}}{Z_{c2}}\sqrt{\frac{\varepsilon_{re1}}{\varepsilon_{re2}}}\right)^2\text{(nH)}$$

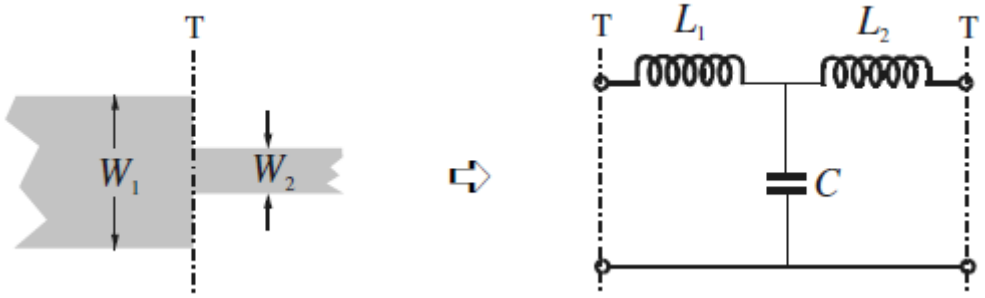

Figure 2.2 Microstrip Discontinuity (Steps in Width)

where L_{wi} for i = 1, 2 are the inductances per unit length of the appropriate micro strips, having widths W1 and W2, respectively. While Z_{ci} and ε_{rei} denote the characteristic impedance and effective dielectric constant corresponding to width Wi, c is the light velocity in free space, and h is the substrate thickness in micrometres.

2.2.2 Open Ends

At the open end of a micro strip line with a width of W, the fields do not stop abruptly but extend slightly further because of the fringing field. This effect can be modelled either with an equivalent shunt capacitance Cp or with an equivalent length of transmission line Δl, as shown

in the following figure. The equivalent length is usually more convenient for filter design. The relation between the two equivalent parameters may be found by

$$\Delta l = \frac{cZ_c C_p}{\sqrt{\varepsilon_{re}}}$$

Where c is the light velocity in free space. A closed-form expression for Δl/h is given by

$$\frac{\Delta l}{h} = \frac{\xi_1 \xi_3 \xi_5}{\xi_4}$$

where

$$\xi_1 = 0.434907 \frac{\varepsilon_{re}^{0.81} + 0.26(W/h)^{0.8544} + 0.236}{\varepsilon_{re}^{0.81} - 0.189(W/h)^{0.8544} + 0.87}$$

$$\xi_2 = 1 + \frac{(W/h)^{0.371}}{2.35\varepsilon_r + 1}$$

$$\xi_3 = 1 + \frac{0.5274 \tan^{-1}[0.084(W/h)^{1.9413/\xi_2}]}{\varepsilon_{re}^{0.9236}}$$

$$\xi_4 = 1 + 0.037 \tan^{-1}[0.067(W/h)^{1.456}] \cdot \{6 - 5 \exp[0.036(1 - \varepsilon_r)]\}$$

$$\xi_5 = 1 - 0.218 \exp(-7.5W/h)$$

The accuracy is better than 0.2% for the range of 0.01 <= w/h <= 100 and ε_r <= 128

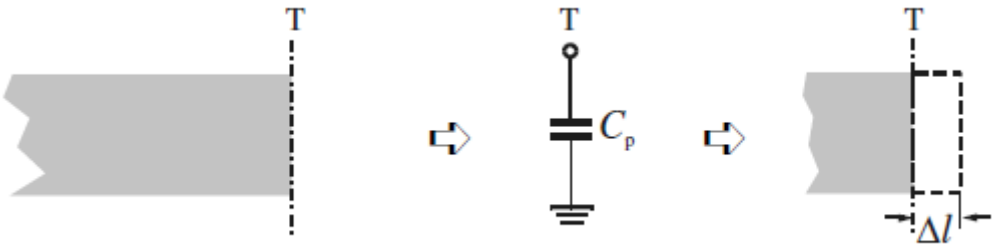

Figure 2.3 Microstrip Discontinuity (Open End)

2.2.3 Gaps

A microstrip gap can be represented by an equivalent circuit, as shown in the following figure. The shunt and series capacitances C_p and C_g may be determined by

$$C_p = 0.5C_e$$

$$C_g = 0.5C_o - 0.25C_e$$

where

$$\frac{C_o}{W}(\text{pF/m}) = \left(\frac{\varepsilon_r}{9.6}\right)^{0.8}\left(\frac{s}{W}\right)^{m_o}\exp(k_o)$$

$$\frac{C_e}{W}(\text{pF/m}) = 12\left(\frac{\varepsilon_r}{9.6}\right)^{0.9}\left(\frac{s}{W}\right)^{m_e}\exp(k_e)$$

with

$$m_o = \frac{W}{h}[0.619\log(W/h) - 0.3853] \qquad \text{for } 0.1 \le s/W \le 1.0$$

$$k_o = 4.26 - 1.453\log(W/h)$$

$$m_e = 0.8675 \qquad \text{for } 0.1 \le s/W \le 0.3$$

$$k_e = 2.043\left(\frac{W}{h}\right)^{0.12}$$

$$m_e = \frac{1.565}{(W/h)^{0.16}} - 1 \qquad \text{for } 0.3 \le s/W \le 1.0$$

$$k_e = 1.97 - \frac{0.03}{W/h}$$

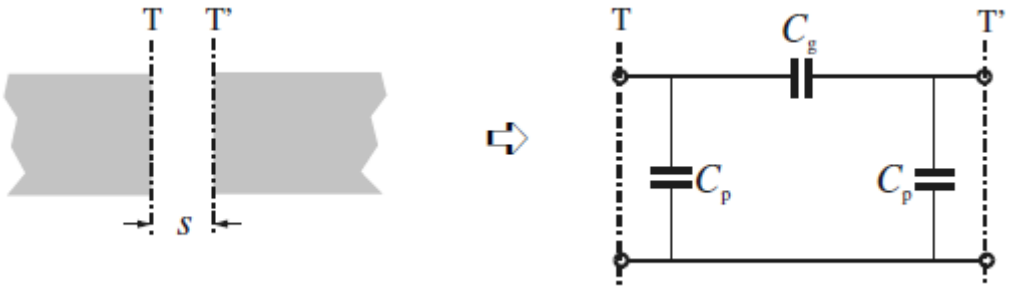

Figure 2.4 Microstrip Discontinuity (Gap)

2.2.4 Bends

Right-angle bends of microstrips may be modeled by an equivalent T-network,as shown in the figure below. The expressions for evaluation of capacitance and inductance is given by:

$$\frac{C}{W}(\text{pF/m}) = \begin{cases} \dfrac{(14\varepsilon_r + 12.5)W/h - (1.83\varepsilon_r - 2.25)}{\sqrt{W/h}} + \dfrac{0.02\varepsilon_r}{W/h} & \text{for } W/h < 1 \\ (9.5\varepsilon_r + 1.25)W/h + 5.2\varepsilon_r + 7.0 & \text{for } W/h \geq 1 \end{cases}$$

$$\frac{L}{h}(\text{nH/m}) = 100\left\{4\sqrt{\frac{w}{h}} - 4.21\right\}$$

The accuracy on the capacitance is quoted as within 5% over the ranges of 2.5 <= ε_r <=15 and 0.1 <= W/h <= 5. The accuracy on the inductance is about 3% for 0.5 <= W/h <= 2.0.

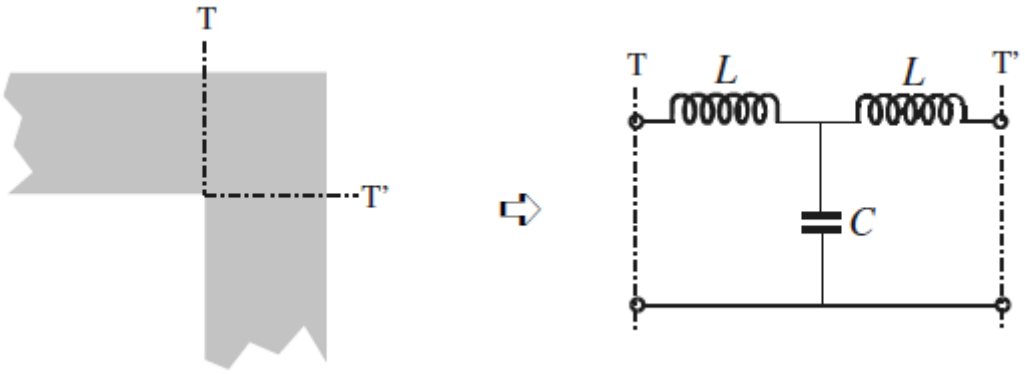

Figure 2.5 Microstrip Discontinuity (Bend)

In the practical designing of the filter these discontinuity concepts are extensively used.

2.3 Quasilumped Elements

Micro strip line short sections and stubs, whose physical lengths are smaller than a quarter of guided wavelength λ_g at which they operate, are the most common components for approximate microwave realization of lumped elements in micro strip filter structures, and are termed quasi lumped elements. They may also be regarded as lumped elements if their dimensions are even smaller, say smaller than $\lambda_g/8$. Some important micro strip quasi lumped elements are discussed in this section.

2.3.1 High- and Low-Impedance Short Line Sections

A short length of high-impedance (Z_c) lossless line terminated at both ends by relatively low impedance (Z_0) is represented by a π-equivalent circuit. For propagation constant $\beta = 2\pi/\lambda_g$ of the short line, the circuit parameters are given by

$$x = Z_c \sin\left(\frac{2\pi}{\lambda_g} l\right) \qquad \text{and} \qquad \frac{B}{2} = \frac{1}{Z_c} \tan\left(\frac{\pi}{\lambda_g} l\right)$$

which can be obtained by equating the ABCD parameters of the two circuits. If $l < \lambda_g/8$ then

$$x \approx Z_c\left(\frac{2\pi}{\lambda_g} l\right) \qquad \text{and} \qquad \frac{B}{2} \approx \frac{1}{Z_c}\left(\frac{\pi}{\lambda_g} l\right)$$

It can be further be shown that for $Z_c >> Z_0$, the effect of the shunt susceptance may be neglected, and this short line section has an effect equivalent to that of a series inductance having a value of $L=Z_c l/v_p$, where $v_p = \omega/\beta$ is the phase velocity of propagation along the short line.

For the dual case shown, a short length of low-impedance (Z_c) loss-less line terminated at either end by relatively high impedance (Z_0) us represented by a T-equivalent circuit with the circuit parameters

$$B = \frac{1}{Z_c} \sin\left(\frac{2\pi}{\lambda_g} l\right) \qquad \text{and} \qquad \frac{x}{2} = Z_c \tan\left(\frac{\pi}{\lambda_g} l\right)$$

For $l< \lambda_g/8$ the values of the circuit parameters can be approximated by

$$B \approx \frac{1}{Z_c}\left(\frac{2\pi}{\lambda_g} l\right) \qquad \text{and} \qquad \frac{x}{2} \approx Z_c\left(\frac{\pi}{\lambda_g} l\right)$$

Similarly, if $Z_c << Z_0$, the effect of the series reactance may be neglected, and this short line section has an effect equivalent to that of a shunt capacitance $C = l/(Z_c v_p)$. To evaluate the quality factor Q of these short-line elements, losses may be included by considering a lossy transmission line with a complex propagation constant $\gamma = \alpha + j\beta$. The total equivalent series resistance associated with the series reactance is then approximated by $R \approx Z_c \alpha l$, whereas the total equivalent shunt conductance associated with the shunt susceptance is $G \approx \alpha l/Z_c$. Since $Q_Z = x/R$ for a lossy reactance element and $Q_Y = B/G$ for a lossy susceptance element, it can be shown that the total Q-factor ($1/Q = 1/Q_Z + 1/Q_Y$) of the short-line elements is estimated by

$$Q = \frac{\beta}{2\alpha}$$

Where β is in radians per unit length and α is in nepers per unit length.

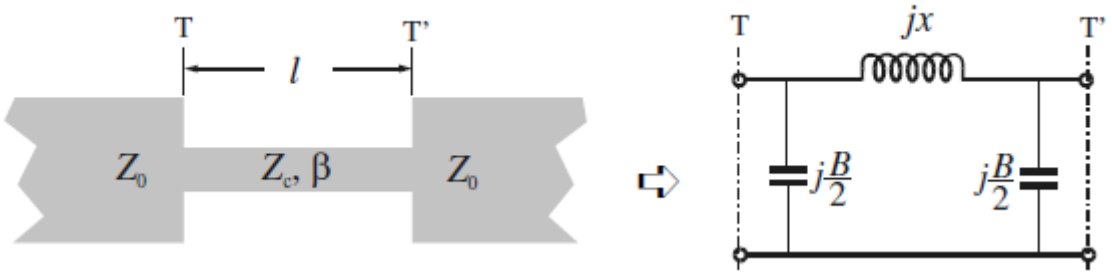

Figure 2.6 High-impedance short-line element

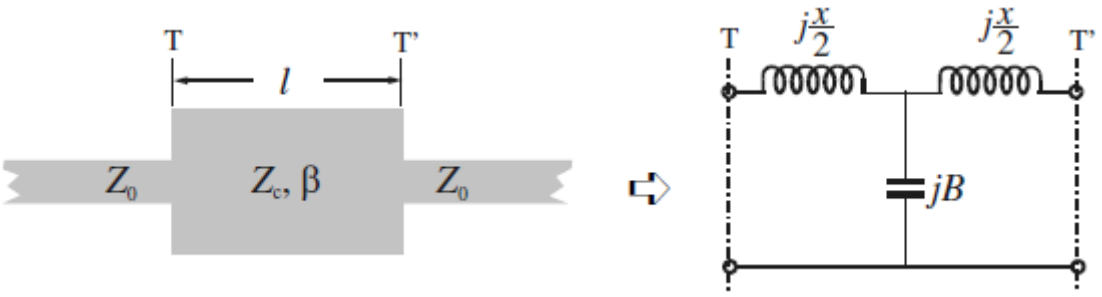

Figure 2.7 Low-impedance short-line element

2.3.2 Open- and Short-Circuited Stubs

We will now demonstrate that a short open circuited stub of lossless micro strip line can be equivalent to a shunt capacitor and that a similar short-circuited stub can be equivalent to a shunt inductor.

According to the transmission line theory, the input admittance of an open-circuited transmission line having a characteristic admittance $Y_c = 1/Z_c$ and propagation constant $\beta = 2\pi/\lambda_g$ is given by

$$Y_{in} = jY_c \tan\left(\frac{2\pi}{\lambda_g} l\right)$$

Where l is the length of the stub. If $l < \lambda_g/4$ this input admittance is capacitive. If the stub is even shorter, say $l < \lambda_g/8$, the input admittance may be approximated by

$$Y_{in} \approx jY_c\left(\frac{2\pi}{\lambda_g} l\right) = j\omega\left(\frac{Y_c l}{v_p}\right)$$

Where v_p is the phase velocity of propagation in the stub. It is now clearer that such a short open-circuited stub is equivalent to a shunt capacitance $C = Y_c l/v_p$. Fo the dual case, the input impedance of a similar short-circuited transmission line is given by

$$Z_{in} = jZ_c \tan\left(\frac{2\pi}{\lambda_g} l\right)$$

This input impedance is inductive for $l < \lambda_g/4$. If $l < \lambda_g/8$, an approximation of the input impedance is

$$Z_{in} \approx jZ_c \left(\frac{2\pi}{\lambda_g} l\right) = j\omega\left(\frac{Z_c l}{v_p}\right)$$

Such a short section of the short-circuited stub functions, therefore, as a shunt lumped-element inductance $L = Z_c l/v_p$.

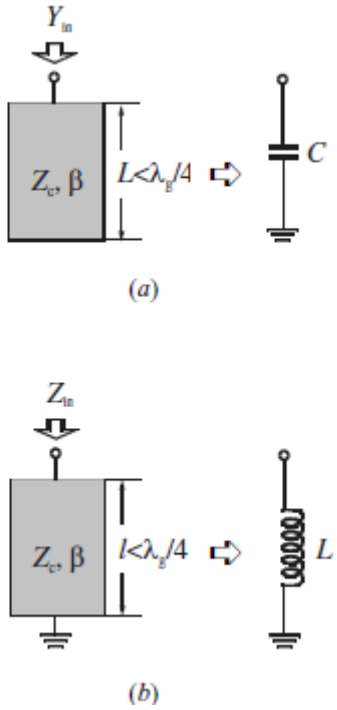

Figure 2.8 Short stub elements: (a) open-circuited stub; (b) short-circuited stub

These stub elements serve as the foundational resonators in the band pass filter design presented later in this work.

2.4 Resonators

A micro strip resonator is any structure that can contain at least one oscillating electromagnetic field. There are numerous forms of micro strip resonators. In general, micro strip resonators for filter designs may be classified as lumped-element or quasi lumped-element resonators and distributed line or patch resonators. Some typical configurations of these resonators are illustrated below.

Lumped-element or quasi lumped-element resonators, formed by the lumped or Quasilumped inductors and capacitors as shown, will obviously resonate at $\omega_0 = 1/\sqrt{LC}$. However, they may

resonate at some higher frequencies at which their sizes are no longer much smaller than a wavelength, and thus, by definition, they are no longer lumped or quasilumped elements. The distributed line resonators shown below may be termed quarter-wavelength resonators, since they are $\lambda_{g0}/4$ long, where λ_{g0} is the guided wavelength at the fundamental resonant frequency f_0. They can also resonate at other higher frequencies when $f \approx (2n - 1) f_0$ for n = 2, 3, · · ·. Another typical distributed line resonator is the half-wavelength resonator, which is $\lambda_{g0}/2$ long at its fundamental resonant frequency, and can also resonate at $f \approx nf_0$ for n = 2, 3, · · ·. In our filter designing these resonating structures play a crucial role.

Figure 2.9 Quarter-wave resonators

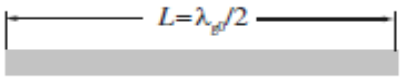

Figure 2.10 Half-wave resonators

The stub-loaded resonators used in this design are based on open-circuited stubs integrated into micro strip line sections to control resonant frequency and bandwidth.

2.5 Scattering Parameters (S-Parameters)

Scattering parameters, or S-parameters, are fundamental tools used to describe the electrical behaviour of high-frequency (microwave and RF) networks. Instead of using voltages and currents directly, S-parameters relate the **incident** and **reflected power waves** at the ports of a device.

For a two-port network:

- **S_{11}**: Input reflection coefficient (how much power is reflected back at port 1)
- **S_{21}**: Forward transmission coefficient (how much power is transmitted from port 1 to port 2)
- **S_{12}**: Reverse transmission coefficient (port 2 to port 1)
- **S_{22}**: Output reflection coefficient (port 2 reflection)

Why Use S-Parameters Instead of Z, Y, or H Parameters?

1. High-Frequency Suitability:

At microwave frequencies, the dimensions of circuits are comparable to the signal wavelengths, and parasitic become significant. Traditional parameters like **impedance (Z)** or **admittance (Y)** are based on **voltage and current**, which are difficult to define and measure precisely in these regimes.

2. Practical Measurement:

S-parameters are measured using a **vector network analyser (VNA)**, which directly measures the magnitude and phase of reflected and transmitted signals (power waves), making them highly convenient and accurate for high-frequency components.

3. Compatibility with Wave Behaviour:

Microwave signals propagate as **electromagnetic waves** through transmission lines, and power wave analysis (as used in S-parameters) better represents this behaviour than circuit theory-based parameters.

4. Port-Based Analysis:

S-parameters naturally fit multi-port devices (e.g., filters, amplifiers, antennas), allowing engineers to easily evaluate performance aspects like:

- **Return Loss** (via S_{11}, S_{22})
- **Insertion Loss** (via S_{21})
- **Isolation** (via S_{12})

5. Passive and Active Device Modelling:

They can describe both **linear passive** (like filters, couplers) and **active** (like amplifiers) components, making them universally applicable in RF and microwave design.

S-parameters are the preferred choice in microwave engineering due to their **measurement practicality**, **suitability for wave-based systems**, and **direct relevance to key performance metrics** in high-frequency circuits.

CHAPTER-3 FILTER DESIGN METHODOLOGY

After discussing all the prerequisites in the first two chapters, this chapter marks the starting of the discussion related to the filter design that is to be practically implemented.

3.1 Problem Statement (Filter Specifications)

The filter design that is to be done is a band pass filter having a passband from 2.625GHz to 5.025 GHz. The filter must have a 0.3dB ripple all over the passband. The insertion loss should be lesser than 2dB while maintaining a return loss lesser than -15dB. The Noise Equivalent Bandwidth (NEB) should be 2400 MHz +- 10%. The stopband rejection (5.550 - 17.25 GHz) should be > 25 dBc. The substrate that is to be used is Alumina (Al_2O_3). The following table shows the entire specification in a tabular format.

Table-1 Filter Specification Detailing

Parameters	Value/Name
Center Frequency	3.825 GHz
0.3dB Bandwidth	2.4 GHz
1 dB Bandwidth	2.450 GHz
Noise Equivalent Bandwidth (NEB) in band of 2 - 17.25 GHz	2400 MHz +- 10%
Insertion Loss	< 2dB
Return Loss	> 15 dB
Stopband Rejection (5.550 - 17.25 GHz)	> 25 dBc
Maximum Substrate Size	1-inch x 1-inch

3.2 Literature Survey

In a previous work [1], 11 order hairpin band pass filter, with Cauer-Chebyshev response designed at C band. The filter is integrated with a harmonic suppression circuit based on quarter-wavelength short stubs. The total circuit has about 1 GHz 3 dB bandwidth at the center frequency of 4.15 GHz. The return loss is better than -12.3 dB and the insertion loss of 2.2 dB in the passband are achieved.

In another work [2], an ultra-wideband band pass filter is designed based on GaAs technology. It is designed by cascading High pass filter (HPF) and Low pass filter (LPF) with a transmission-zero out band rejection method. The two filters are designed with 5^{th} order Chebyshev approach separately and then cascaded to get the desired band pass filter. To have a fast roll-off attenuation, out-of-band transmission zero is applied. Thus a parallel resonance

circuit is used. Moreover, L-network impedance matching has been introduced to improve the input return losses. The resultant size is 3.23 mm^2 with 1.2 dB insertion loss, 134.6% fractional bandwidth, and 16.2 dB return loss.

Work [3] represents another UWBPF with four transmission zeros and seven poles. It consists of series transformers, coupled lines, and a shunt-stepped impedance open stub. The even-odd mode analysis method and scattering parameters theory. The center frequency is of 2.496 GHz, designed, simulated, and tested. The measured 3 dB fractional bandwidth is 103.2%, and the fabricate prototype occupies an area of 0.165 λ_g^2.

Work [4] presents a very sharp rejection band pass filter (BPF) design techniques in suspended substrate strip line (SSS). The proposed band pass filter is split into two parts viz., high pass filter (HPF) and low pass filter (LPF) and both are designed separately in SSS and integrated by providing slight matching between two and made a single circuit. The same generalized Chebyshev LPF prototype has been considered for both the design. Then Richard's frequency transformation is applied to map the LPF prototype to LPF as well as HPF respectively in distributed domain using commensurate transmission lines. Then Kuroda's identities applied to flip the elements in the shunt branch of HPF. This design technique also redistributes (n-3) finite transmission zeroes into different frequency zones near the cut-off frequency ($\pm\omega_0$) to maintain rejection hump better than 100 dB at both the side of the BPF.

Work [5] presents a compact quadruple-mode ultra-wideband (UWB) band pass filter with sharp selectivity and extremely wide upper stopband is proposed in this paper, using a multi-stage stepped impedance resonator, two open-circuited ends and a pair of high low impedance stubs. The characteristics of the proposed multimode resonator are analysed by simulation, demonstrating that the first four resonant modes can be appropriately located in the desired passband and other resonant modes in the upper stopband can be suppressed. To improve the skirt selectivity and out-of-band performance, two identical high-low impedance stubs are introduced into the design, without changing any resonant characteristic of the filter. Finally, the improved filter is fabricated and measured, and simulated and measured results are in good agreement to show that the proposed filter has a sharp selectivity with a -21.5 dB rejection stopband extended to over 30 GHz.

3.3 Theoretical Approach

Before approaching the practical designing process, theoretical calculations are done to choose the type of response, order of the filter which can cater all the constraints.

3.3.1 Substrate Analysis

The design is implemented on an Alumina (Al_2O_3) substrate, which is a commonly used ceramic material in RF and microwave circuits due to its excellent electrical and mechanical properties. Below mentioned are some of the key substrate parameters:

- Substrate Height (H): 25 mils (0.635 mm)
- Relative Dielectric Constant (ε_r): 9.9
- Loss Tangent (Tan D): 0.0007

- Conductor Material: Gold (Au)
- Conductor Thickness (T): 8 um
- Conductivity: 4.1E+7
- Upper Housing Height (Hu): 11 mm
- Substrate Area: 1-inch x 1-inch

Alumina is selected as the dielectric substrate for its high permittivity ($\varepsilon_r = 9.9$), which enables miniaturization of the resonator structures and helps achieve compact layout within the given area constraint of 1 inch × 1 inch. Its low loss tangent (0.0007) is ideal for microwave frequencies, contributing to low insertion loss and improved quality factor (Q).

The conductor material is gold, which, although slightly less conductive than copper, is chosen for its excellent surface conductivity, resistance to oxidation, and stable performance over time, especially beneficial at high frequencies where the skin effect confines current to the surface. The 8 µm thickness ensures adequate conduction while maintaining fine patterning precision. The 11 mm upper housing height is considered in EM modelling to account for shielding and possible cavity resonance effects.

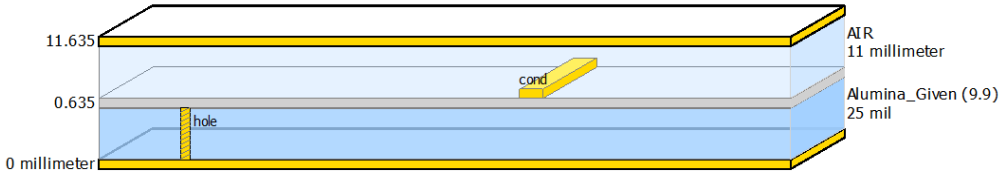

Figure 3.1 Substrate structure used for design

3.3.2 Filter Design Analysis

At first to satisfy the given filter specifications, both Butterworth and Chebyshev responses are tried out. After hit and trial process the Chebyshev response is selected. In case of Chebyshev, the 0.3dB specification refers to the passband ripple. Now the process is to determine the order of the filter to design the prototype low pass filter at first. Below show all the initial calculations done.

Order of the filter (n):

$$n \geq \frac{cosh^{-1}\sqrt{\frac{10^{0.1L_{As}}-1}{10^{0.1L_{Ar}}-1}}}{cosh^{-1}(\frac{\omega 1}{\omega c})}$$

Here one considerations is taken for getting the normalised filter element values for Chebyshev Response, the values are taken from predefined tables mentioned in [6]. In that the passband

ripple L_{Ar} is considered is around 0.1 dB instead of 0.3 dB which is closest to our required specification.

After putting the values, we get the filter order to be approximately a 7^{th} order filter. Now it different design topologies are to explored to satisfy our requirement.

Filter topology selection:

The filter topology selection totally depends upon the given filter specifications and Fractional Bandwidth (FBW) of the required filter. The Fractional Bandwidth can be calculated from the given formulae:

$$FBW = \frac{\omega_2 - \omega_1}{\omega_0}$$

where,

$$\omega_0 = \frac{\omega_1 + \omega_2}{2}$$

After putting the value of ω_1, ω_2, and ω_0 the computed Fractional Bandwidth (FBW) is around 62.74%. Catering to this along with other filter specifications Open-Stub Topology is considered because of the following reasons:

- Wide Fractional Bandwidth Handling

Open-stub topologies are inherently well-suited for wideband responses. Unlike narrowband resonator designs (e.g., coupled lines or hairpins), open stubs allow more flexibility in shaping the frequency response over large bandwidths with controlled return loss and ripple.

- High Design Compactness

With a high dielectric constant substrate ($\varepsilon_r = 9.9$) and small layout constraint (1 inch × 1 inch), open-stub filters can achieve greater miniaturization. The quarter-wavelength stubs can be tightly packed or meandered while maintaining their electrical length, enabling a compact layout without compromising performance.

- Low Insertion Loss Potential

Open stubs, when implemented with high-quality conductors like gold, exhibit very low conductor loss due to minimal discontinuities and short line sections. Combined with the low-loss Alumina substrate, this supports specification of insertion loss < 2 dB.

- Good Return Loss Performance

The Chebyshev-based open-stub design can be tuned to achieve the required return loss < -15 dB across the passband. Matching networks at input/output can further optimize VSWR without excessive complexity.

- Simplicity of EM Simulation and Tuning

Open-stub filters are relatively easy to model and simulate using full-wave EM tools. Their performance can be fine-tuned by adjusting stub lengths and spacing, without needing complex 3D structures or multilayer configurations.

- Flexibility in Topology Variations

Open stubs can be configured in shunt, series, or pseudo-lumped forms, and can easily integrate with other filter sections or impedance matching networks. This makes them flexible for integration into broader microwave systems.

There arises a question why some of the potential topologies like Parallel Coupled Line Filters, Hairpin Filter. This can be answered based on the following points:

- Large Size for Wide Bandwidth

Both coupled-line and hairpin filters are inherently suited for narrowband applications. Your design requires a wide fractional bandwidth (~63%), which would force these topologies to use large spacing and long resonators, making it difficult to fit within your 1 inch × 1 inch area constraint.

- Tight Coupling Requirements

Achieving wide bandwidth with coupled lines requires very tight spacing between lines—often <0.1 mm. This violates your minimum separation constraint (0.1 mm) and is hard to fabricate reliably.

- Complex Layout and Tuning

Hairpin filters involve bent $\lambda/2$ resonators and become geometrically inefficient at wide bandwidths. The layout becomes large and complex, making EM tuning and optimization harder, especially on a high-ε_r substrate like Alumina, where lines shrink but coupling becomes more sensitive.

- Poor Size-to-Performance Trade-off

Compared to open-stub designs, both coupled-line and hairpin filters would require larger physical dimensions for the same bandwidth, while also offering no significant advantage in insertion loss or return loss under your specifications.

So, the conclusion of the theoretical analysis is to design a 7^{th} order Chebyshev Filter using open stub topology. In the following section, the design parameters are mentioned along with the calculated dimensions, and responses both from the schematic and layout.

3.4 Practical Implementation

As computed from the theoretical analysis the design is supposed to be a 7th order BPF having a Chebyshev Response. First there are certain formulae that are needed to be used for computing the lengths and thickness of the stubs

$$\theta = \frac{\pi}{2}\left(1 - \frac{FBW}{2}\right)$$

$$h = 2$$

$$\frac{J_{1,2}}{Y_0} = g_0\sqrt{\frac{hg_1}{g_2}}, \qquad \frac{J_{n-1,n}}{Y_0} = g_0\sqrt{\frac{hg_1g_{n+1}}{g_0g_{n-1}}}$$

$$\frac{J_{i,i+1}}{Y_0} = \frac{hg_0g_1}{\sqrt{g_ig_{i+1}}} \qquad \text{for } i = 2 \text{ to } n-2$$

$$N_{i,i+1} = \sqrt{\left(\frac{J_{i,i+1}}{Y_0}\right)^2 + \left(\frac{hg_0g_1\tan\theta}{2}\right)^2} \qquad \text{for } i = 1 \text{ to } n-1$$

$$Y_1 = g_0Y_0\left(1 - \frac{h}{2}\right)g_1\tan\theta + Y_0\left(N_{1,2} - \frac{J_{1,2}}{Y_0}\right)$$

$$Y_n = Y_0\left(g_ng_{n+1} - g_0g_1\frac{h}{2}\right)\tan\theta + Y_0\left(N_{n-1,n} - \frac{J_{n-1,n}}{Y_0}\right)$$

$$Y_i = Y_0\left(N_{i-1,i} + N_{i,i+1} - \frac{J_{i-1,i}}{Y_0} - \frac{J_{i,i+1}}{Y_0}\right) \qquad \text{for } i = 2 \text{ to } n-1$$

$$Y_{i,i+1} = Y_0\left(\frac{J_{i,i+1}}{Y_0}\right) \qquad \text{for } i = 1 \text{ to } n-1$$

Here Y_i means the characteristic admittance of the stubs and $Y_{i,i+1}$ refers to the characteristic admittance of the connecting lines between the stubs. It is to be noted that the electrical length of the open stubs is $\lambda_g/2$. The above shown equations are same for both open stub as well as short circuited stubs. There are two more formulae that we must consider which are now specifically required for open circuited stub filter design:

$$Y_{ia} = \frac{Y_i(\alpha_i \tan^2 \theta - 1)}{(\alpha_i + 1)\tan^2 \theta}$$

$$Y_{ib} = \alpha_i Y_{ia}$$

Where,

$$\alpha_i = \cot^2\left(\frac{\pi f_{zi}}{2f_0}\right) \qquad \text{for } f_{zi} < f_1$$

Basically, these two formulae are used to convert any $\lambda_g/4$ short-circuit stub filter into $\lambda_g/2$ open-circuit stub filter. Y_{ia} and Y_{ib} refers to the characteristic admittance of each $\lambda_g/4$ stubs which are connected in series with each other to get the required $\lambda_g/2$ open-circuited stubs. If in some case $Y_{ia} = Y_{ib}$ then the stopband will have attenuation poles at the frequencies $f_0/2$ and $3f_0/2$. However, if $Y_{ib} = \alpha Y_{ia}$, then the attenuation poles can be made to occur at frequencies other than $f_0/2$ and $3f_0/2$. This is the case in our scenario, because of which we do have additional passband in the vicinity of f=0 and $f=2f_0$.

In our case the calculated value of α_i=0.866, as a result the connected $\lambda_g/4$ are not equal. Also, the calculated value of λ_g is 31.77 mm at our center frequency of 3.825 GHz, along with ε_{re} being 6.0963.

3.4.1 7th Order Open-Stub Filter Design

The following table consists of all the computed admittances and the corresponding impedances.

Table-2 Computed values for 7th order Open-Stub Filter

i	Y_i	$Y_{i, i+1}$	Z_i	$Z_{i, i+1}$
1	0.0252	0.0258	39.6825	38.7597
2	0.0496	0.0274	20.163	36.4964
3	0.0495	0.026	20.202	38.4615
4	0.0502	0.026	19.9203	38.4615
5	0.0495	0.0274	20.202	36.4964
6	0.0496	0.0258	20.163	38.7597
7	0.0252		39.6825	

Schematic View:

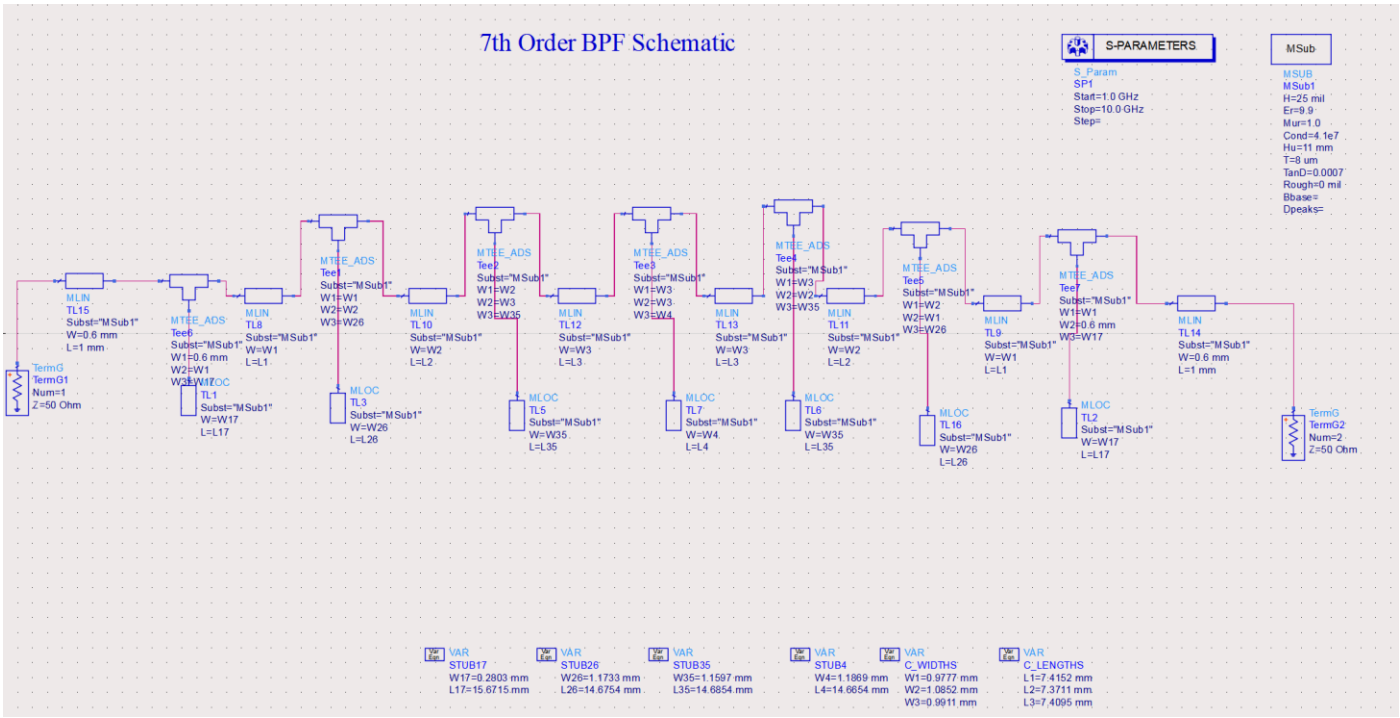

Figure 3.2 Schematic representation of the 7th order filter

Schematic Simulation Result:

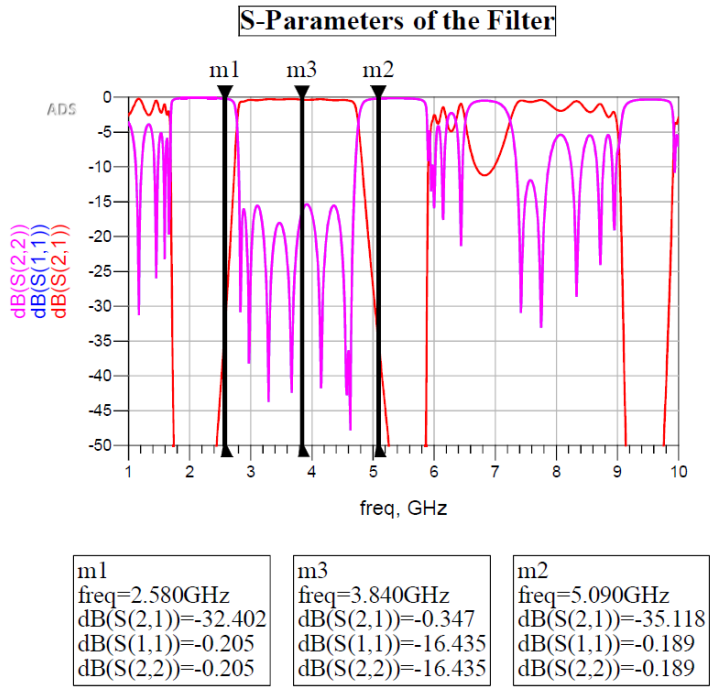

Figure 3.3 S-Parameters from schematic simulation

As from the schematic simulation it is observed that the result is not what should have happened, so for a better representation the layout simulation is performed whose results are shown below.

Layout View:

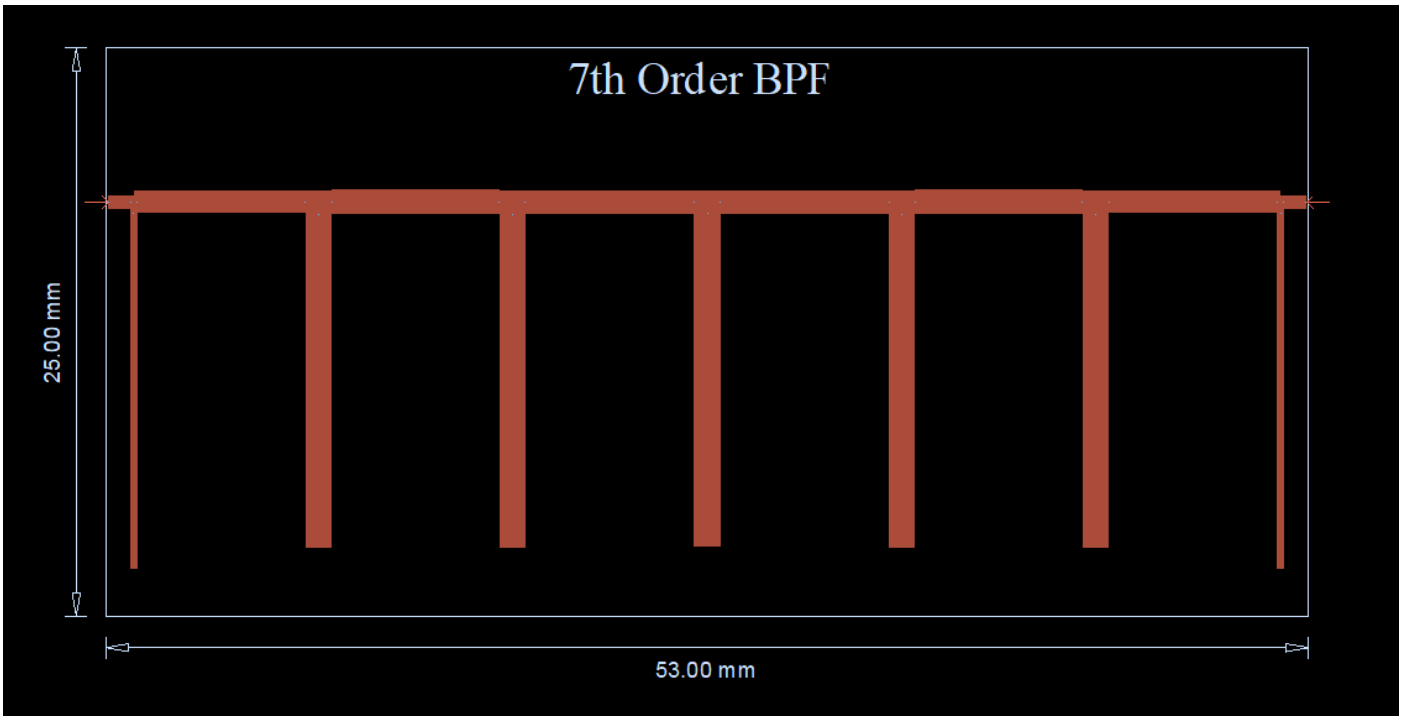

Figure 3.4 Layout representation of 7th order filter

Layout Simulation Result:

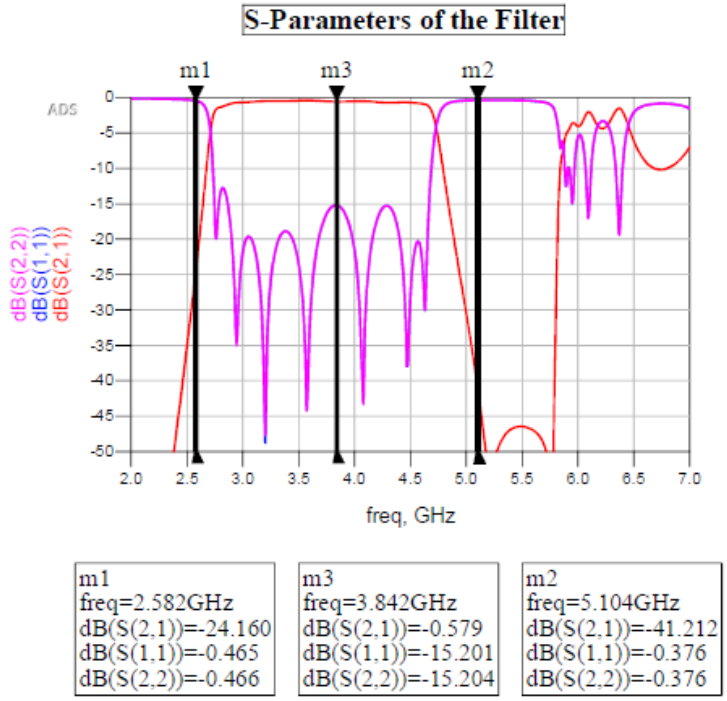

Figure 3.5 S-Parameters from layout simulation

Observation: Even from the layout simulation, it is observed the result does not satisfy the specification needed. Also, it is observed that the layout is not coming under the 1-inch x 1-inch substrate criteria.

Conclusion: As a result, any further attempt for optimisation is not performed on this design.

It is to be considered that because of lack of some specs required to design any filter, there are assumptions that are made because of which the calculated also needs some hit and trial approach. Following this there are two other order of filters that are designed: 6^{th} order and 5^{th} order.

3.4.2 6^{th} Order Open-Stub Filter Design

Every calculation procedure remains the same, the main change occurs in the computational values, which is because of the change in the normalised filter element values that too because of the change in the order of the filter.

Table-3 Computed values for 6^{th} order Open-Stub Filter

i	Y_i	$Y_{i, i+1}$	Z_i	$Z_{i, i+1}$
1	0.0248	0.0258	69.4444	38.7597
2	0.0487	0.0275	35.4610	36.3636
3	0.0484	0.0265	35.7143	37.7358
4	0.0484	0.0275	35.7143	36.3636
5	0.0487	0.0258	35.4610	38.7597
6	0.0248		69.4444	

Schematic View:

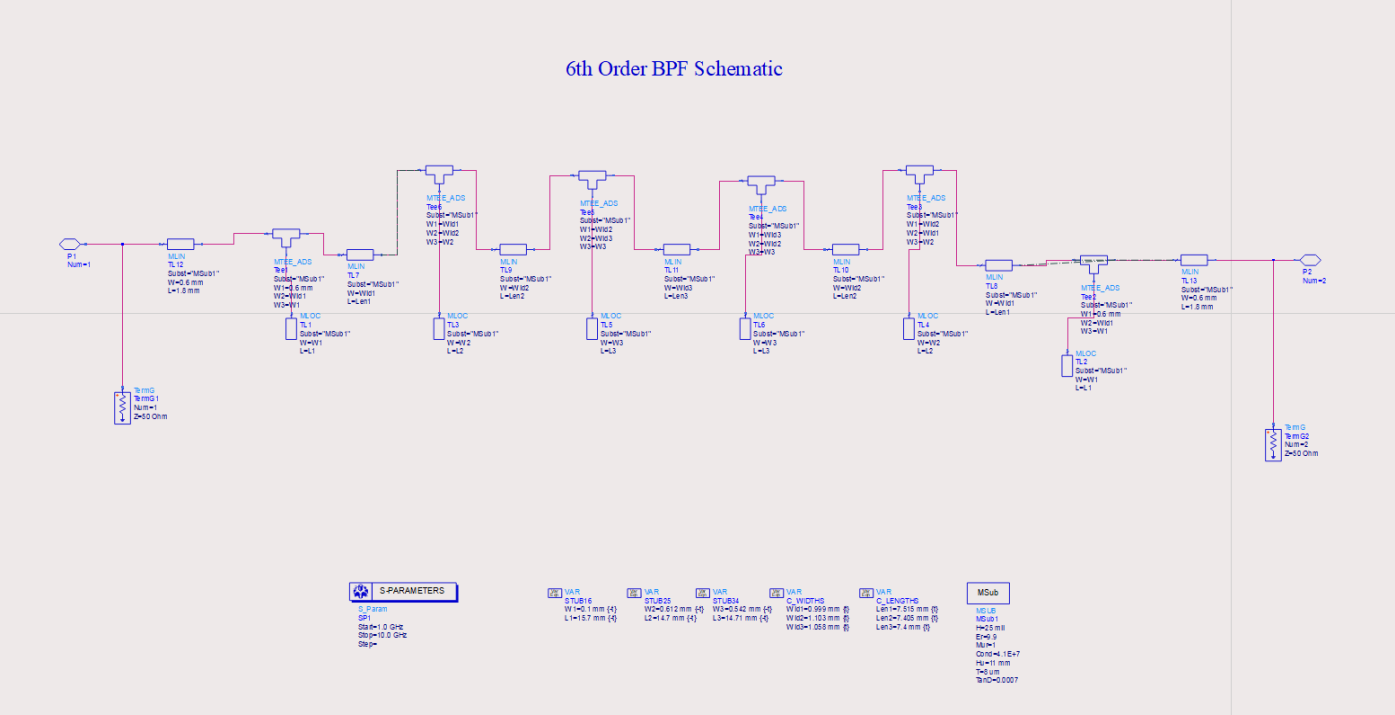

Figure 3.6 Schematic representation of 6th order filter

Schematic Simulation Result:

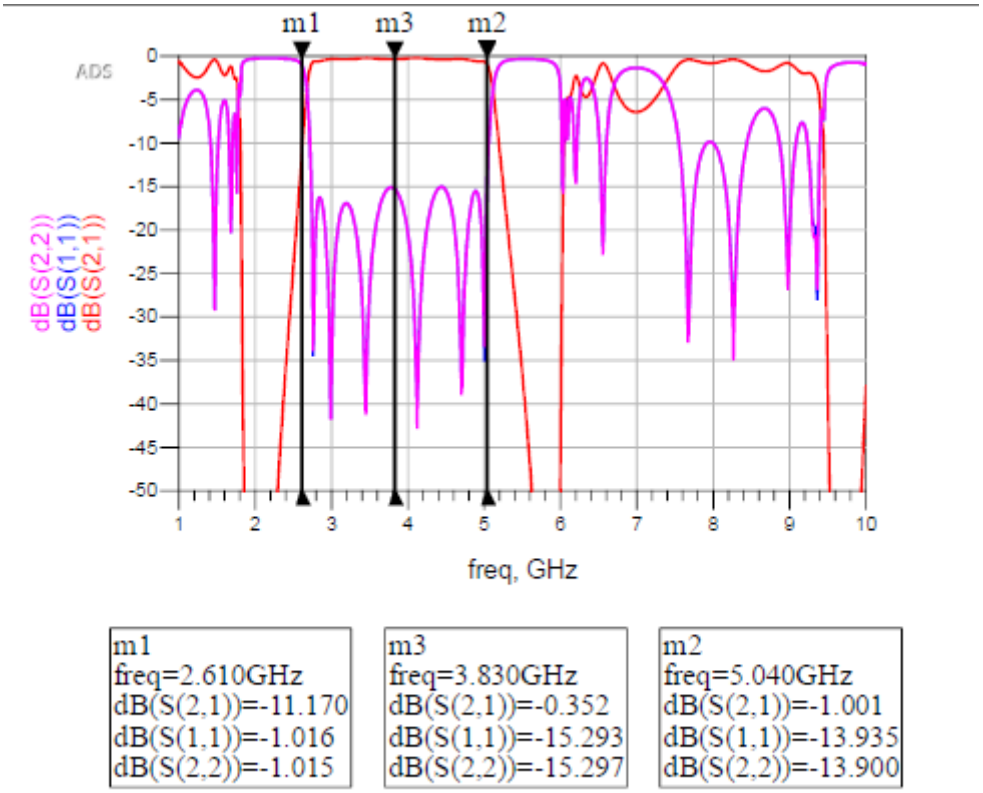

Figure 3.7 S-Parameters from schematic simulation (6th order)

The schematic simulation response for the 6th order filter improves from that of the 7th order filter. However there the response does not fully satisfy at the lower end of the passband. Again, the directly converted layout simulation is done to see the actual response of the filter.

Layout View:

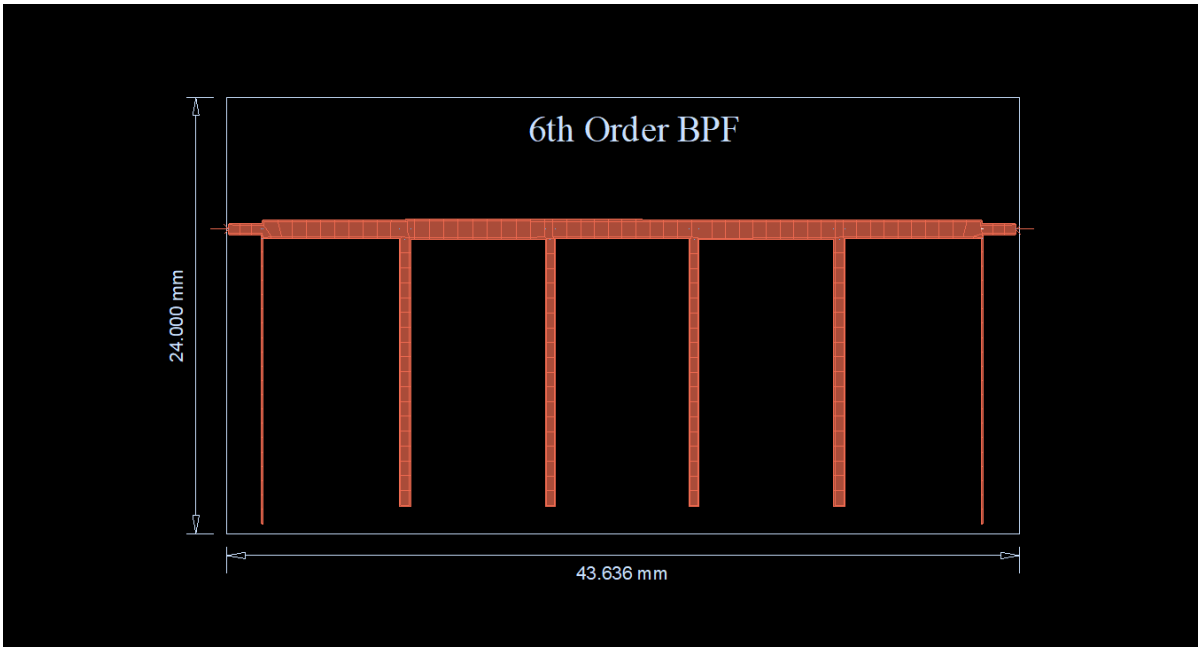

Figure 3.8 Layout representation of 6th order filter

Layout Simulation Result:

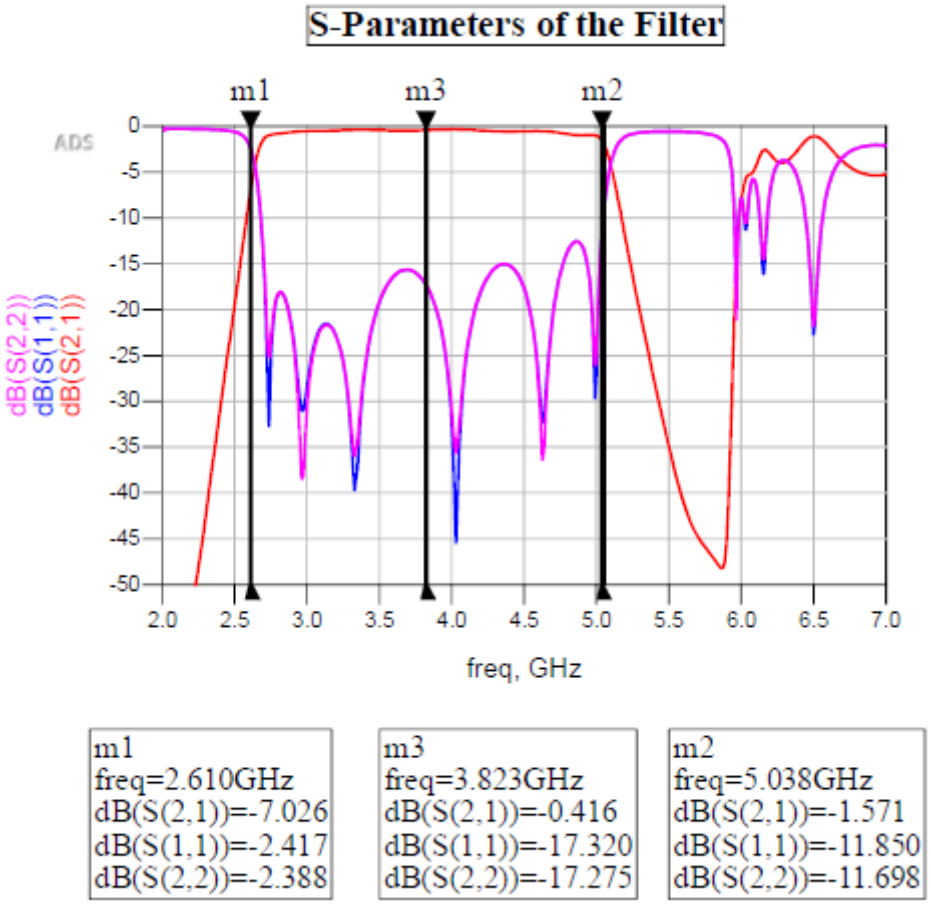

Figure 3.9 S-Parameters from layout simulation (6th order)

Observation: The layout simulation does show that the design covers a better portion of the passband than that of the 7th order filter however it is observed that the S11 parameter worsens from the layout simulation of that of 7th order filter. Infact the layout can again further be optimised to even fit for the substrate area constraint.

Conclusion: Several other bend types are tried maintaining the topology while trying to fit the area constraint. There also it is to be considered that the input port and the output port should be always parallel to each other to meet the system constraint. Following this criterion several bend iterations are done, but none helps in maintaining the specification mentioned and does not improve the S11 response along with the shrinkage in the passband.

After trying both the 7th and 6th order filter, it is observed that the response improved with lower order filter size considering the assumptions that are made along with the provided specifications.

3.4.3 5th Order Open-Stub Filter Design

Following the hit and trial method, a 5th order filter is also designed and it is observed that it can satisfy most of the specifications that are provided. In this design also the measurements are done separately while maintaining the same α_i value and same ε_{re}.

Table-4 Computed values for 5th order Open-Stub Filter

i	Y_i	$Y_{i, i+1}$	Z_i	$Z_{i, i+1}$
1	0.0241	0.0259	71.4286	38.61
2	0.0472	0.0279	36.7647	35.8423
3	0.0462	0.0279	37.4532	35.35.8423
4	0.0472	0.0259	36.7647	38.61
5	0.0241		71.4286	

Schematic View:

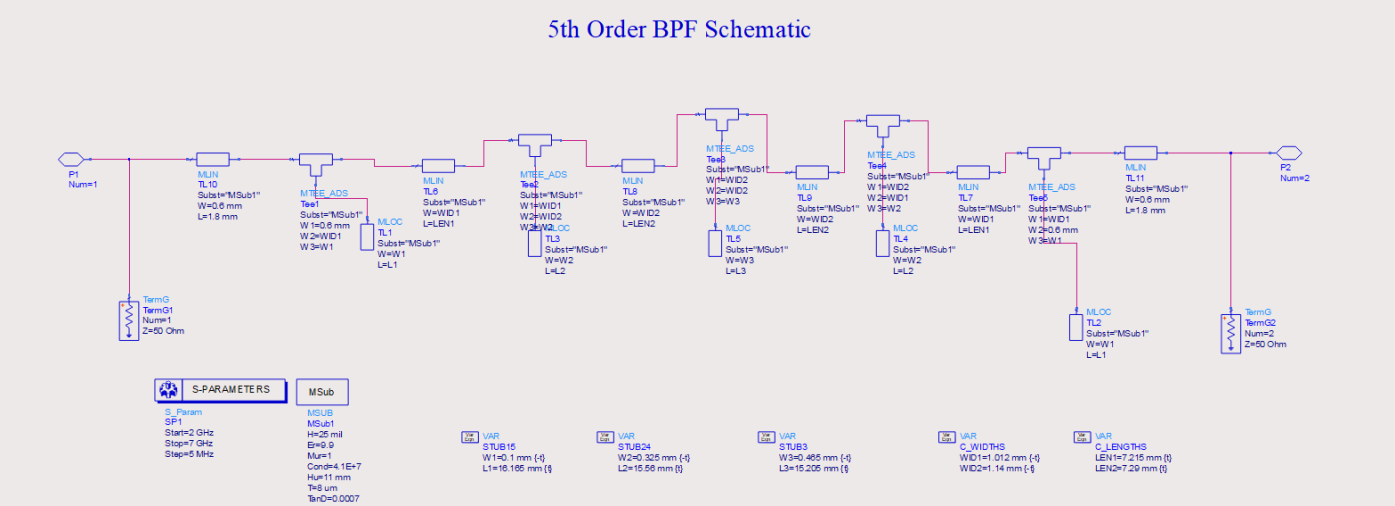

Figure 3.10 Schematic representation of 5th order filter

Schematic Simulation Result:

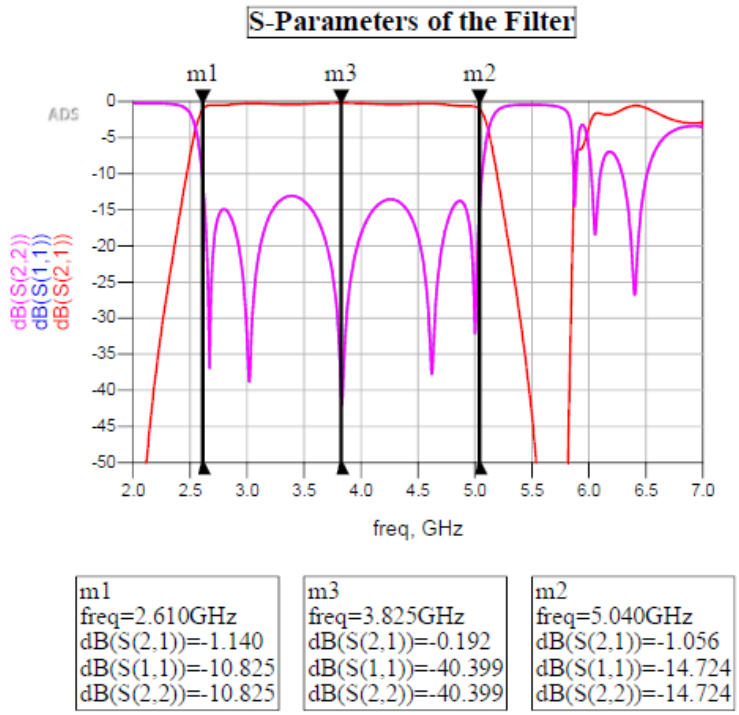

Figure 3.11 S-Parameters from schematic simulation (5th order)

The schematic simulation shows promising results, satisfying most of the specifications with some minor tunings. For a better visualisation of the response, the default generated layout is simulated.

Layout View:

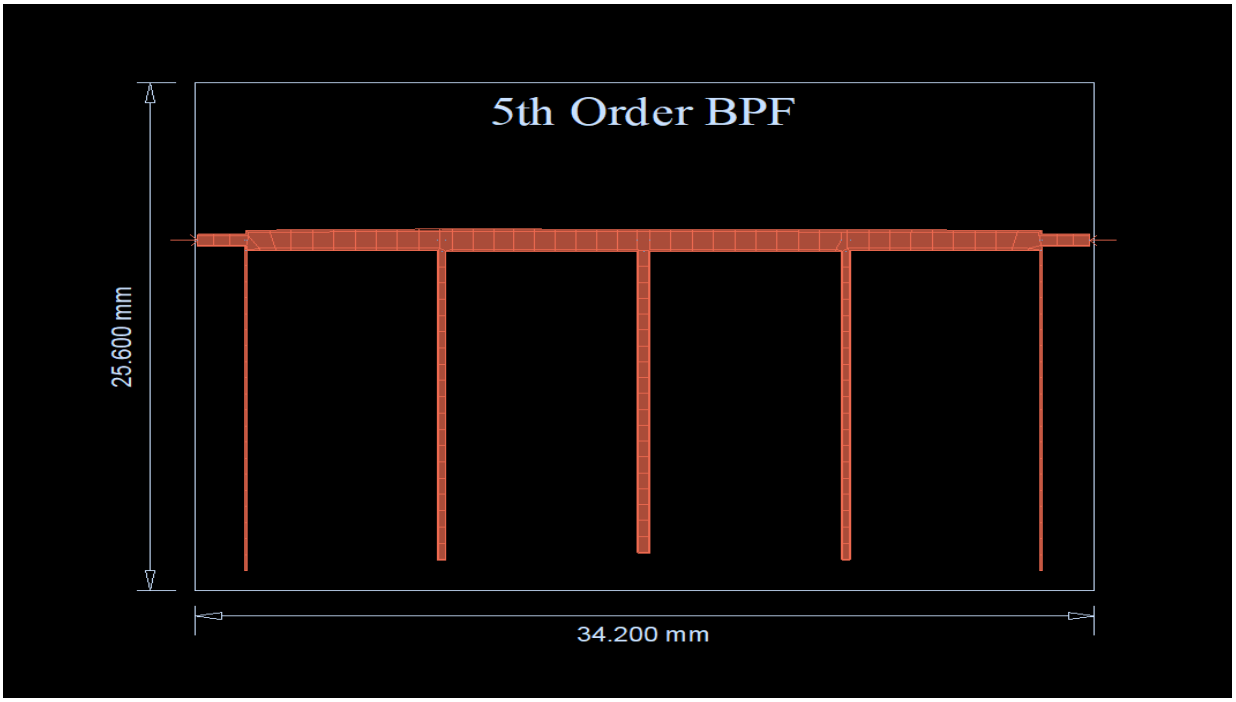

Figure 3.12 Layout representation of 5th order filter

Layout Simulation Result:

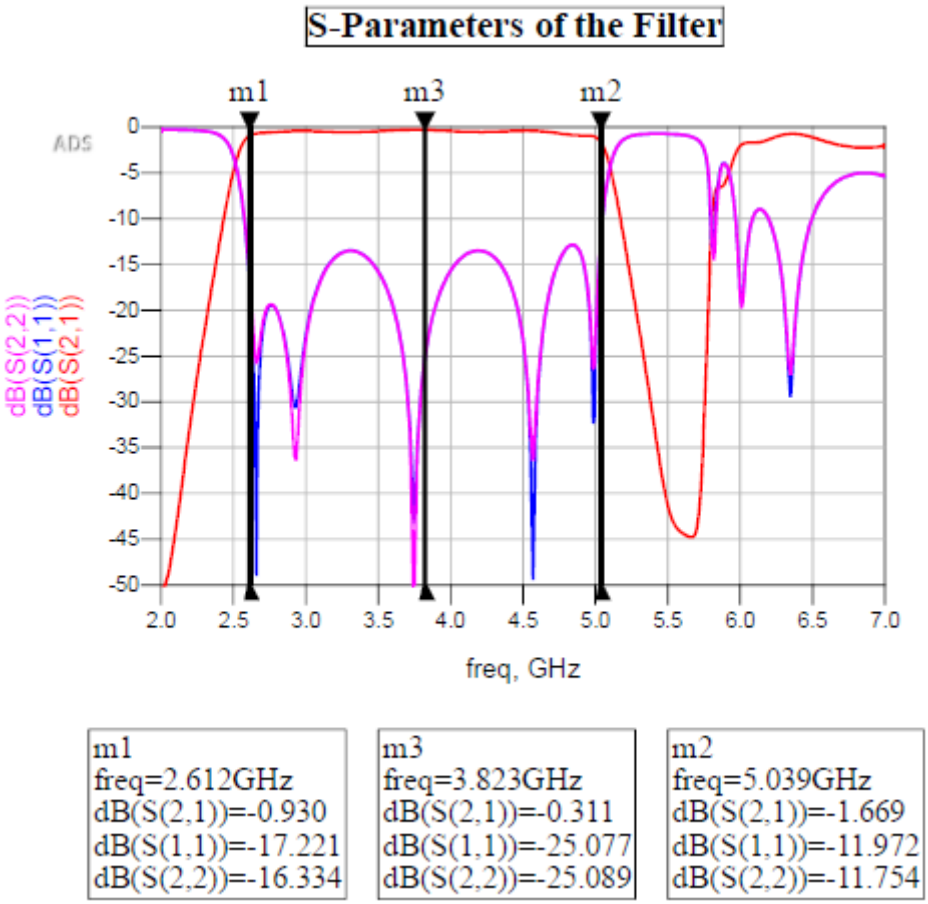

Figure 3.13 S-Parameters from schematic simulation (5th order)

Observation: The simulated result from the default generated layout also shows promising results satisfying most of the given specifications as well, without doing any major changes and the size of the filter is comparable in accordance to the substrate size mentioned.

Conclusion: The default layout for the 5^{th} order filter shows the best response among all the three orders that are tried. Also, there is scope of making the design compact to satisfy the substrate area constraint.

The finalised order satisfying our all assumptions practically is a 5^{th} order BPF, now there several hit and trial iterations mostly on bending the structure to satisfy the constraints provided, some of which are shown below.

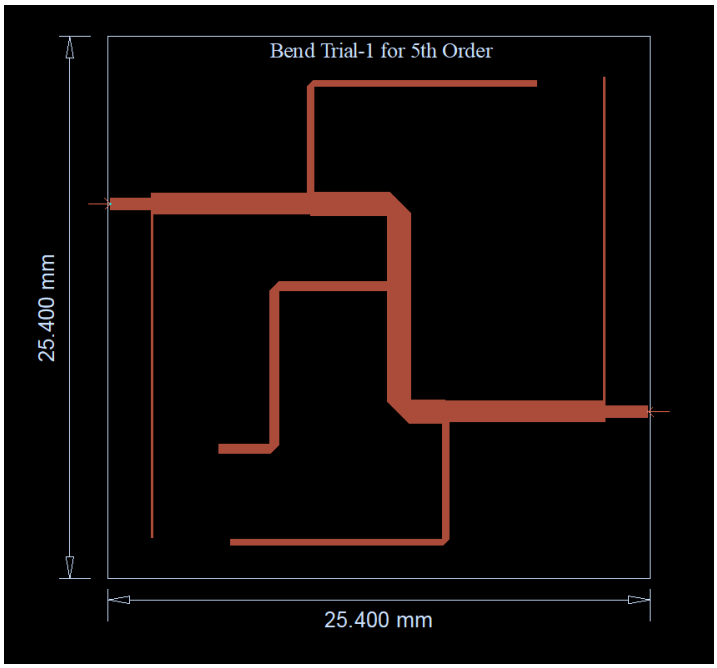

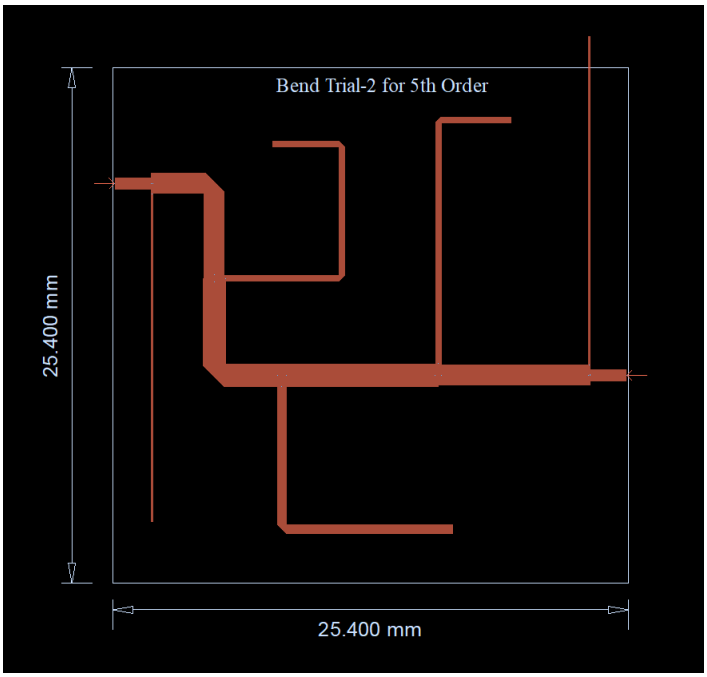

Figure 3.14 Bend trial optimisations for 5th order filter

The above figures show two of the trial bends for optimisation of the filter. Here all the bends are done with a mitering ratio of 45%.

A small test is performed before further optimisation where the insertion loss and return loss both are checked with respect to the mitering ratio which varies from 30% to 65%. The design and responses are shown below.

Layout View:

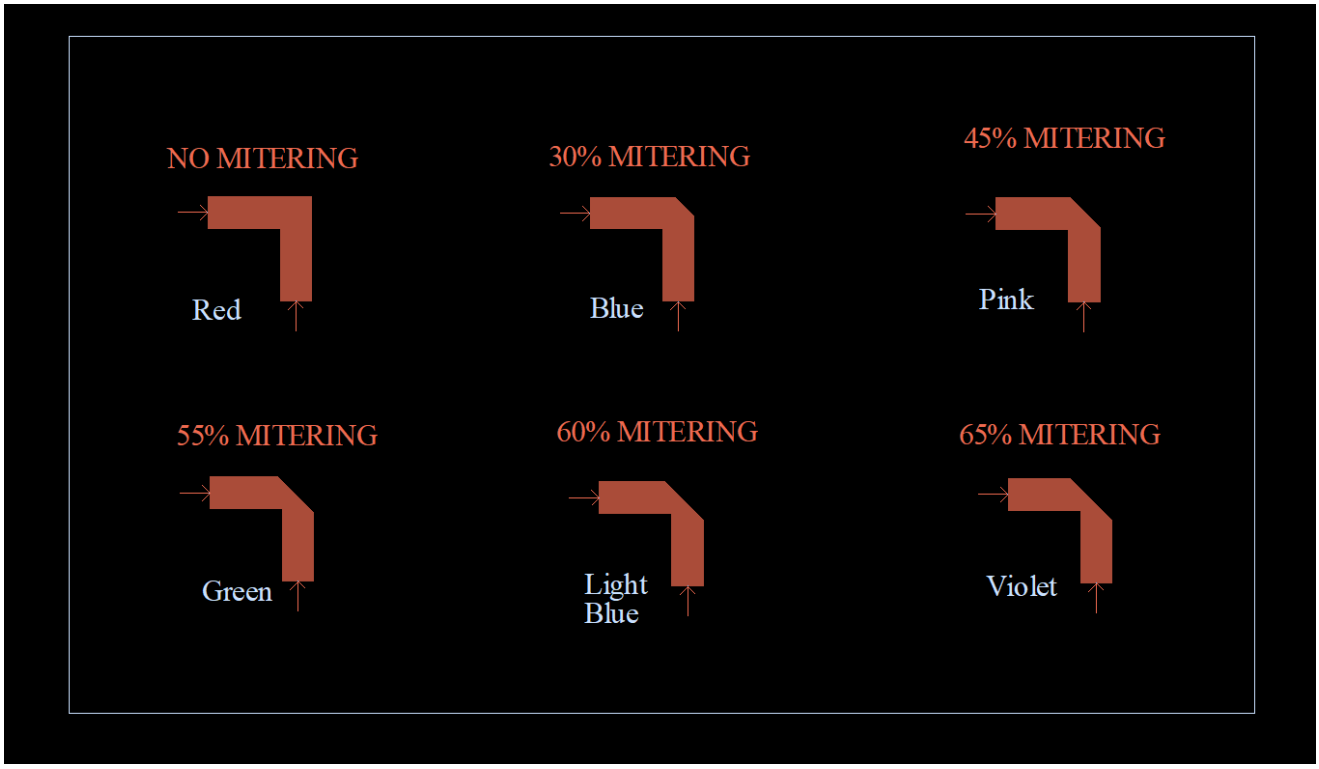

Figure 3.15 Different mitering ratios

Layout Simulation View:

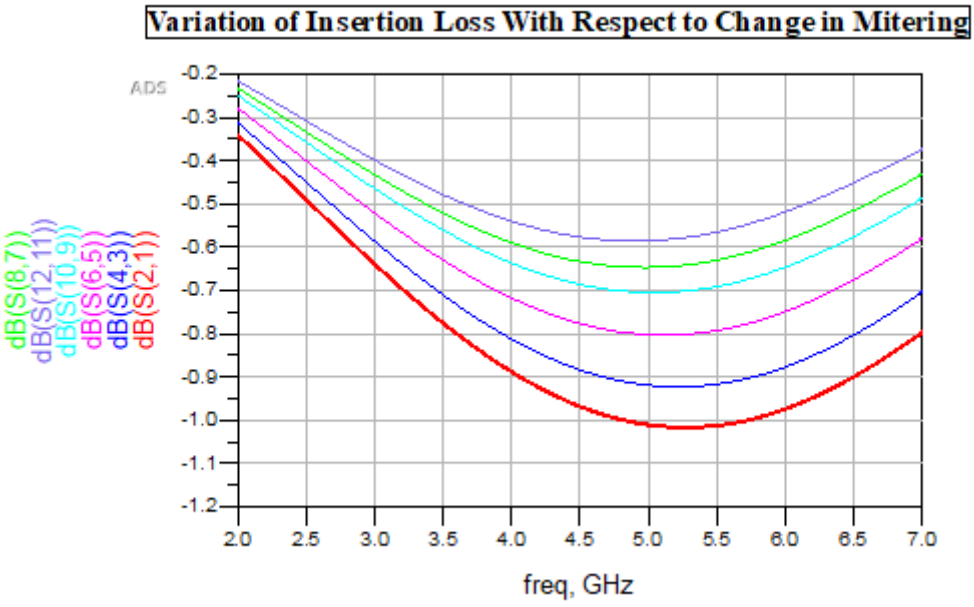

Figure 3.16 Variations of insertion loss

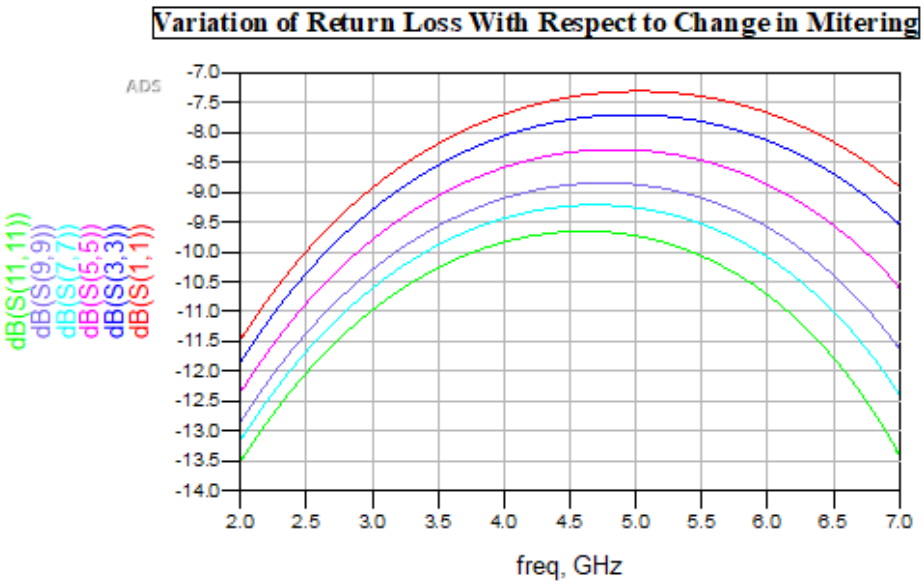

Figure 3.17 Variations of return loss

From the above simulated results, it is observed that the mitering ratio of 65% performs the best in comparison to other mitering ratios. The choice of the mitering ratio needs to be carefully done to make the design feasible for fabrication purpose.

3.4.4 Optimised 5th Order Open-Stub Filter Design

After changing the mitering ratio again multiple bend trials are performed among which the below design trial comes to be the most optimised design.

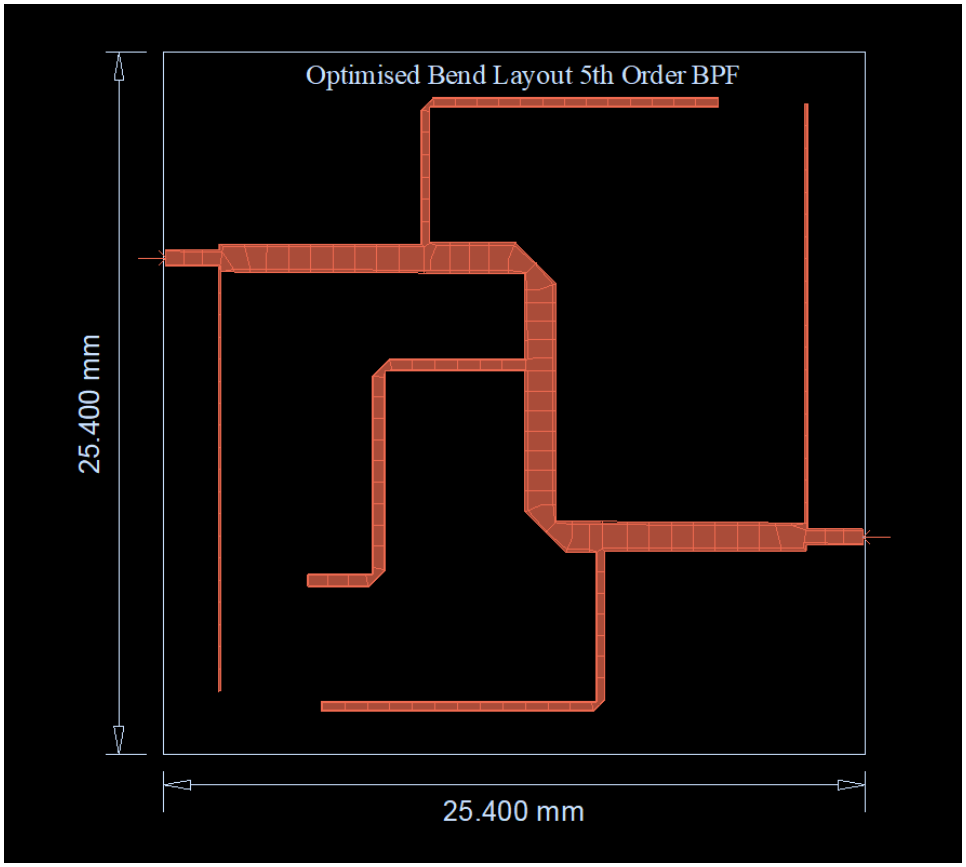

Figure 3.18 Optimised layout for the 5th order filter design

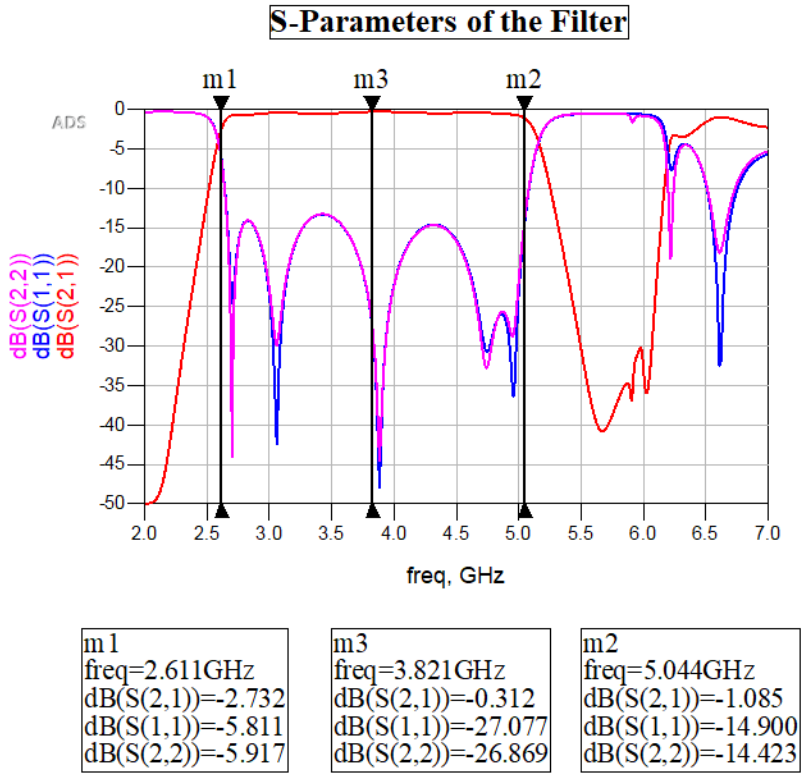

Figure 3.19 S-Parameters from layout simulation

3.4.5 Final Optimised 5th Order Open-Stub Filter Design

As can be seen from the above response, the S-Parameters improved a lot by using a mitering ratio of 65%, this ratio has been selected in accordance with the fabrication feasibility. However, the above design is not perfect and needs to be optimised slightly in order to get the exact response, also there is an issue of extra passband (harmonic) that needs to be removed while keeping the entire design limited within the 1-inch square substrate area. For these reasons slight modifications have been done in the filter, including changes in the bend position and bend type. The final optimised design is shown on the next page along with all the responses.

Layout View:

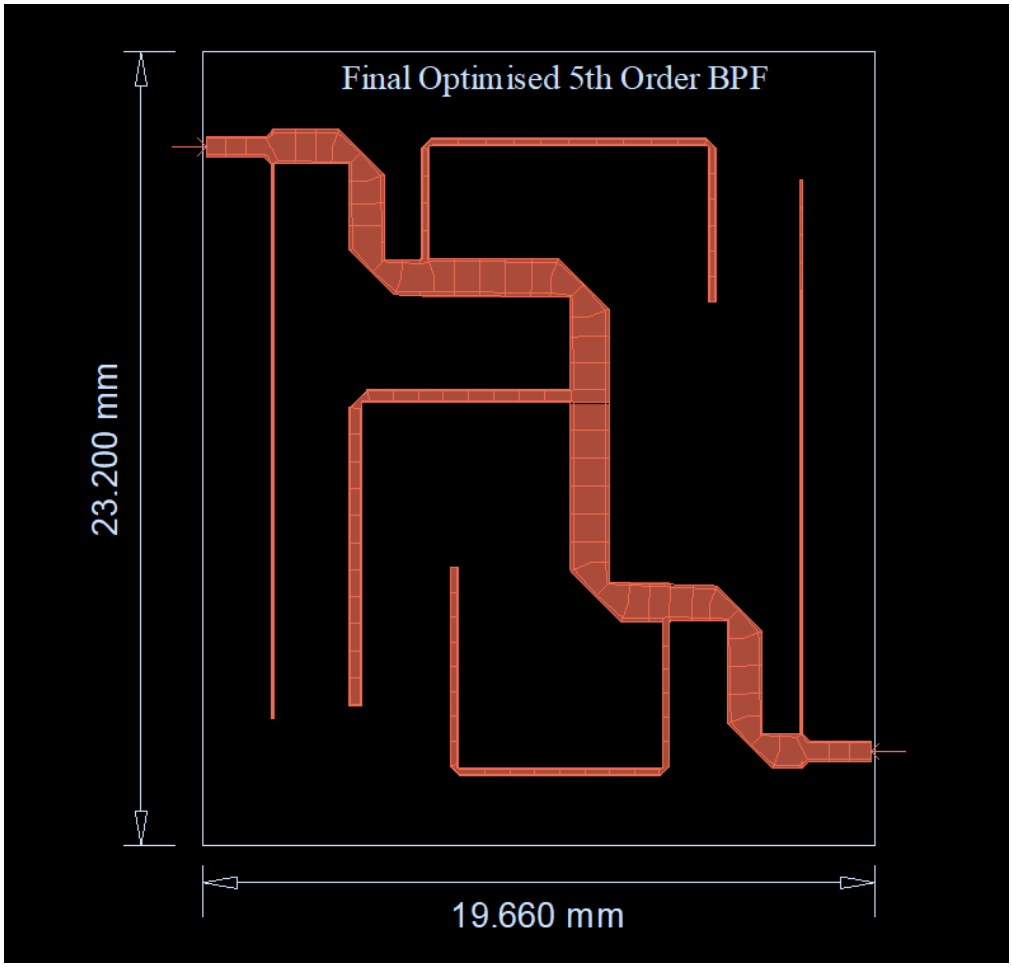

Figure 3.20 Final optimised layout for 5th order filter

Layout Simulation Result:

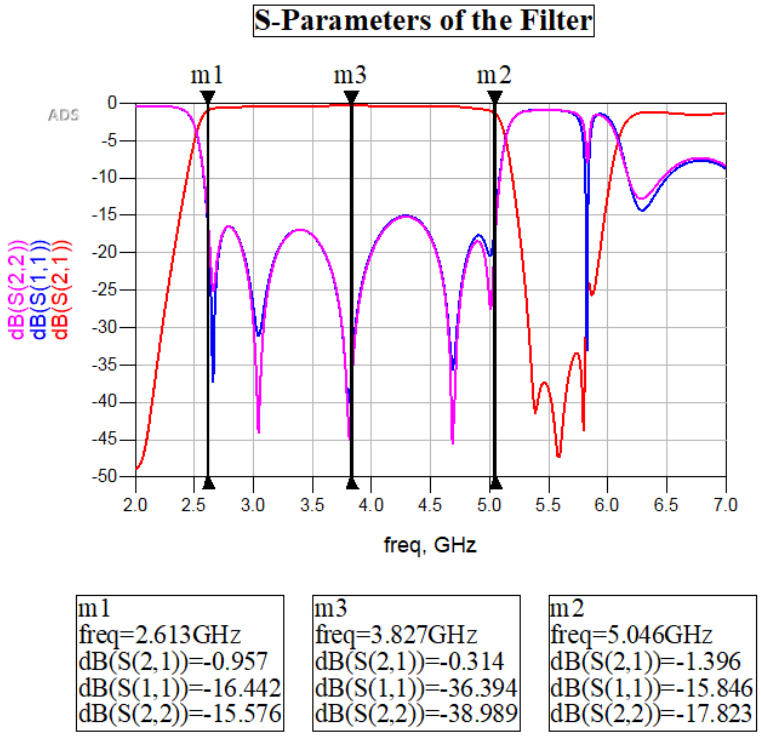

Figure 3.21 S-Parameters from final optimised layout simulation

Observation: The S-Parameter response satisfies all the specifications that are required, and also the optimised result is obtained at smaller size than that of the substrate size.

Conclusion: The designed BPF can be used to successfully, however there is a small issue that needs to be fixed which refers to the presence of extra passband occurring beyond the desired passband.

3.5 Design Challenge

Challenge: As from the simulated result shown above it is observed that the designed band pass filter alone passes not only the desired passband but also some extra sidebands that occurs beyond f= $f_0/2$ and f = $3f_0/2$. The reason behind this is the inequality in Y_{ia} and Y_{ib}. This is a serious issue as it will severely affect the filter response and the Noise Equivalent Bandwidth (NEB). This is one of the main trade-offs for open-stub filter design.

Solution: To solve this problem the filter needs to relate suitable HRF (Harmonic Rejection Filter) and a HPF.

The HRF is designed to eliminate the response beyond the upper limit of our passband i.e. 5.025GHz.

3.5.1 Theoretical Approach

We considered to design a HRF having a 3dB cut-off at 5.3 GHz along with passband ripple (L_{Ar}) of around 0.1 dB while giving a stopband rejection of 30dB at 6.2GHz.

Order of the filter (n): The order of the filter is selected to be 7^{th} order as that satisfies most of our required specification.

The characteristic impedances for thin and thick line are 90 Ω and 20 Ω respectively. Correspondingly, the widths of the lines are calculated to be 0.12 mm and 1.96 mm respectively.

Also the λ_g are calculated for both the thin and thick micro strip lines by considering the different ε_{reff} obtained from LineCalc toolchain.

Finally, the length of the thin and thick micro strip lines representing the inductor and capacitor are calculated using the given two formulae:

$$l_{Ln} = \frac{g_n Z_0 \lambda_h}{2\pi Z_h}$$

$$l_{Ln} = \frac{g_n Z_l \lambda_l}{2\pi Z_0}$$

The first formula is for micro strip line representing inductor while the second formula is for one that represents capacitor.

Table-5 Computed values for 7th order Harmonic Rejection Filter

Element	Width (mm)	Length (mm)
L1	0.12	2.1
L2	0.12	0.4
C2	1.96	1.94
L3	0.12	3.24
L4	0.12	1.19
C4	1.96	1.58
L5	0.12	2.53
L6	0.12	1.19
C6	1.96	0.84
L7	0.12	0.90

3.5.2 Practical Approach

After calculating all the dimensions, the schematic of the respective HRF is designed along with it simulated S-Parameter result.

Schematic View:

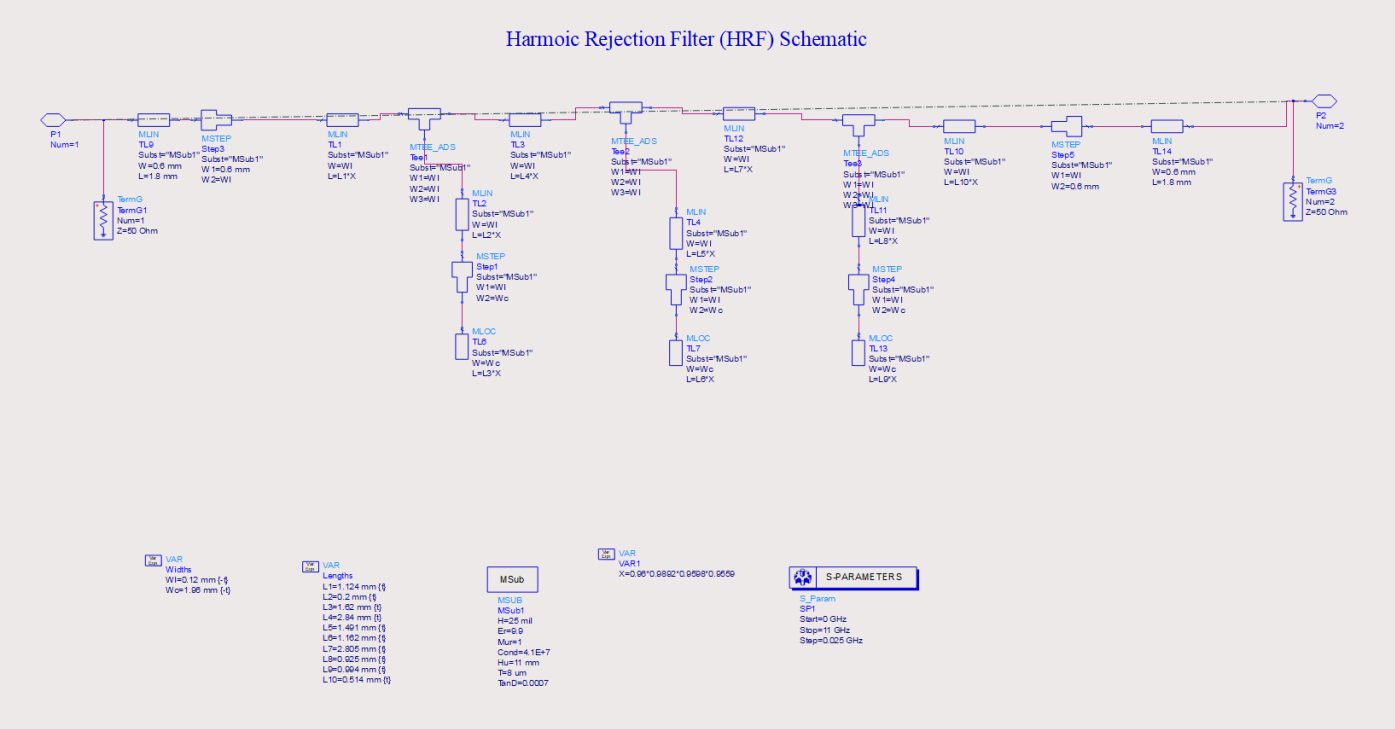

Figure 3.22 Schematic representation of 7th order harmonic rejection filter (HRF)

Schematic Simulation Result:

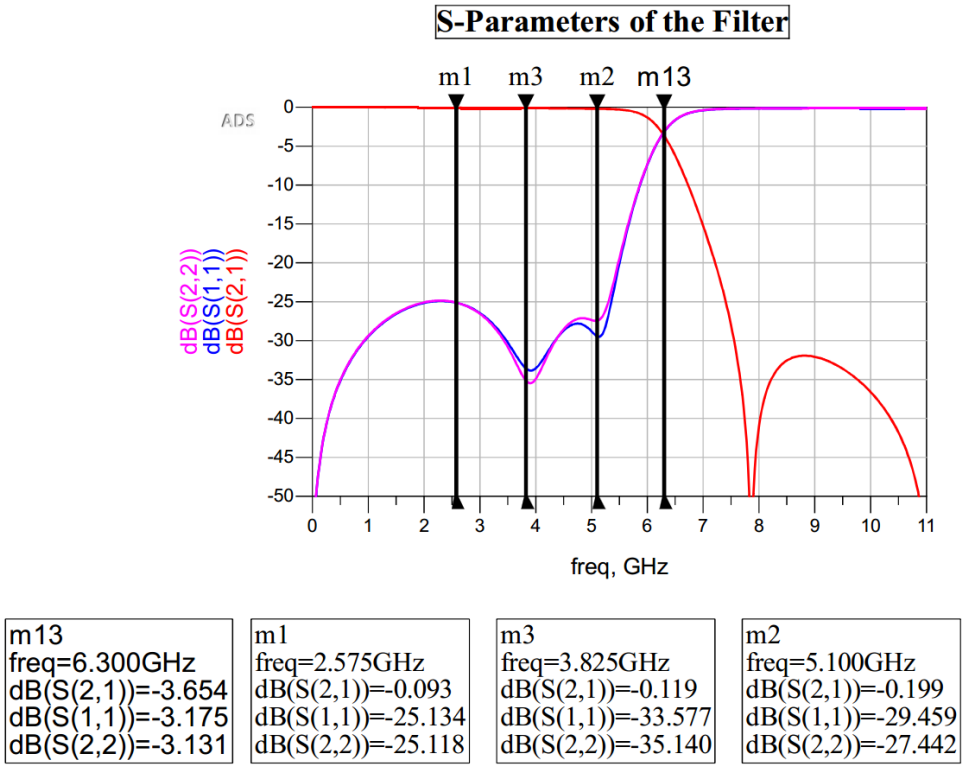

Figure 3.23 S-Parameters from schematic simulation of 7th order HRF

As from the simulation result, it is observed that the schematic response shifts the 3dB cut-off from 5.3 GHz to 6.3 GHz. This has been to practically adjust the response of the filter. The dimensions of all the above computed values are changed by an adjusting factor ‘m’ which is calculated by the ratio of the practical 3dB cut-off point to the schematic 3dB cut-off point. To get the practical response of the filter, layout simulation is done.

Layout View:

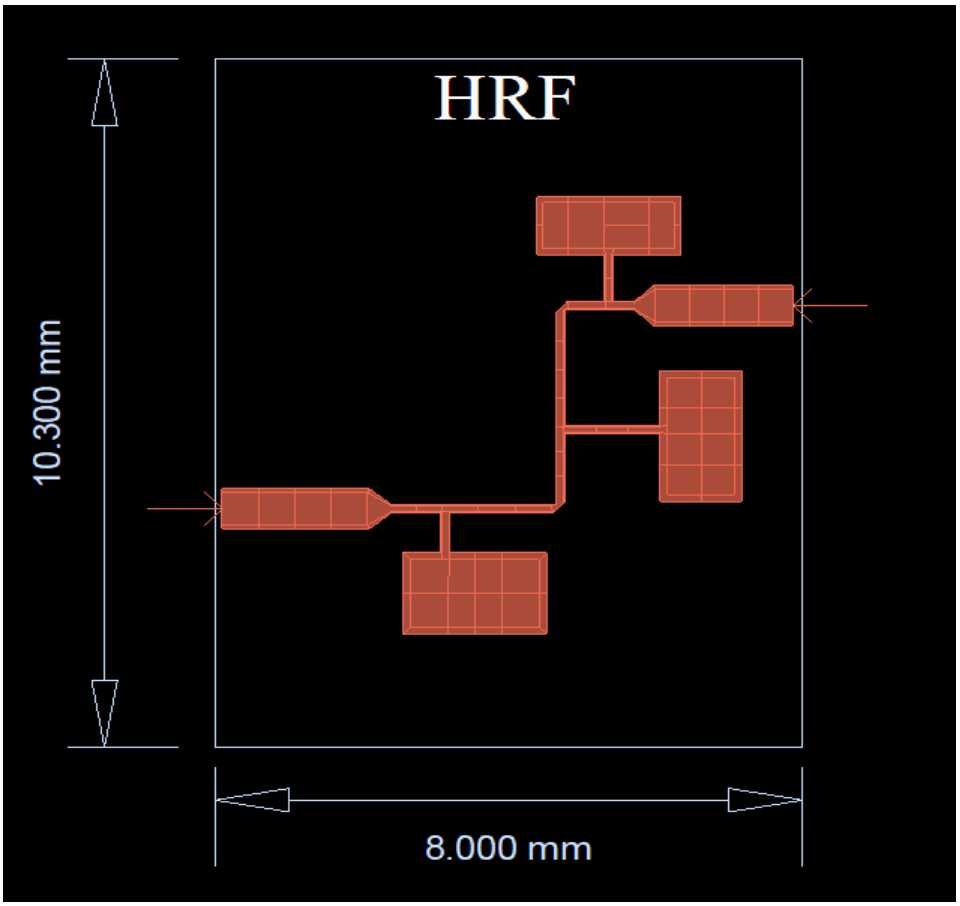

Figure 3.24 Layout representation of 7th order harmonic rejection filter (HRF)

Layout Simulation Result:

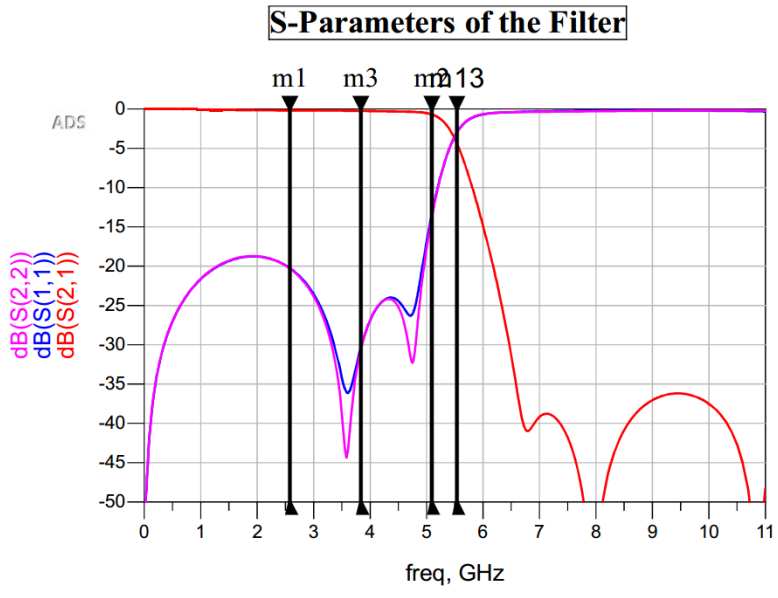

m13 freq=5.538GHz dB(S(2,1))=-4.415 dB(S(1,1))=-3.010 dB(S(2,2))=-2.974	m1 freq=2.578GHz dB(S(2,1))=-0.187 dB(S(1,1))=-20.252 dB(S(2,2))=-20.299	m3 freq=3.836GHz dB(S(2,1))=-0.250 dB(S(1,1))=-30.310 dB(S(2,2))=-30.575	m2 freq=5.093GHz dB(S(2,1))=-0.693 dB(S(1,1))=-13.402 dB(S(2,2))=-13.776

Figure 3.25 S-Parameters from layout simulation of 7th order HRF

Observation: The layout response of the harmonic rejection filter satisfies all the required specifications along with optimisation in its size for satisfying the substrate area constraint.

Conclusion: The designed layout can successfully be integrated with the BPF and can actually be fitted under the 1-inch x 1-inch size.

After finalising the design of both the BPF and HRF, the needs two needs to be integrated into a final layout, whose response is to be recorded. One of the challenging issue is the impedance mismatch that occurs in-between the two filters, that is needed to be fixed.

3.5.3 Co-Simulation Results

Co-simulation is performed to optimise the impedance mismatch, two structures are performed, one is a T-section and the other is a stepped-junction.

Co-Simulation 1 View:

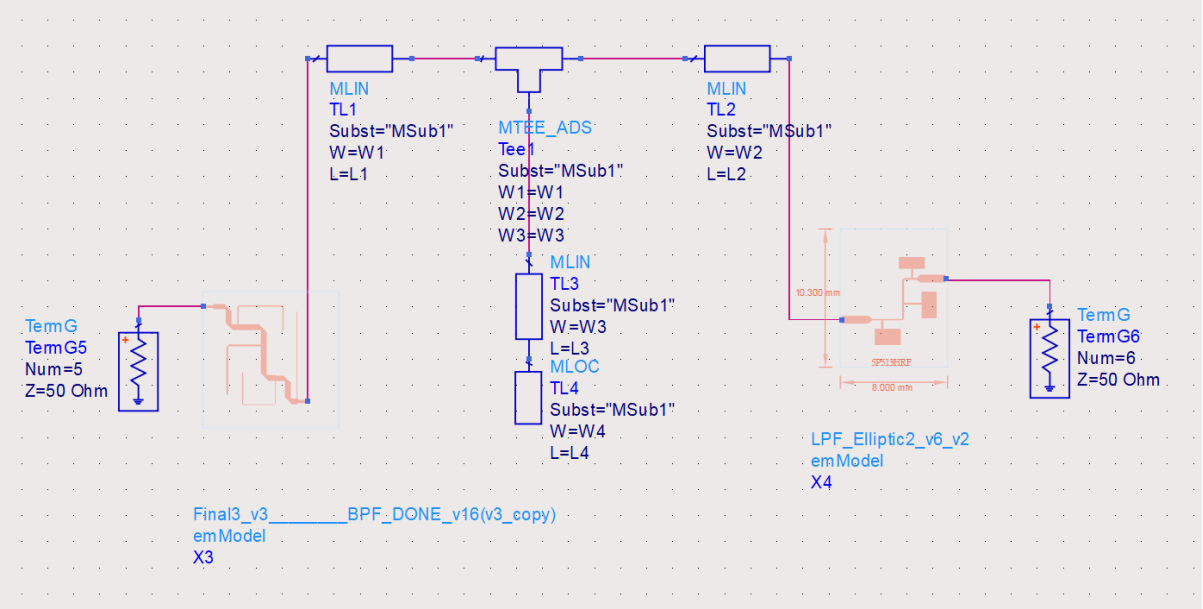

Figure 3.26 Co-simulation for impedance matching using T-section

Co-Simulation 1 Response:

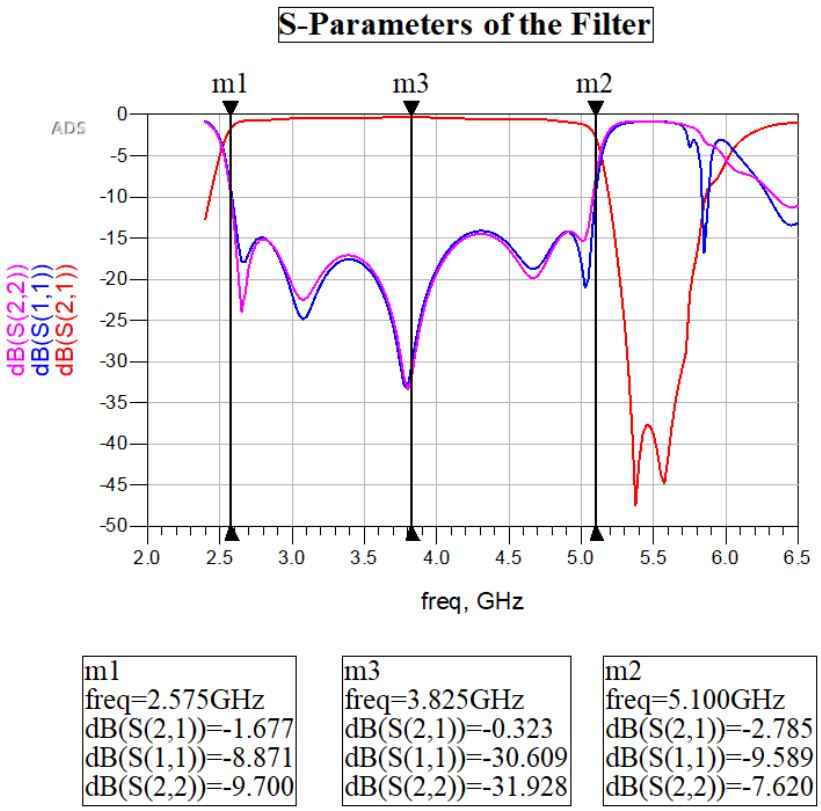

Figure 3.27 S-Parameters from co-simulation 1

Co-Simulation 2 View:

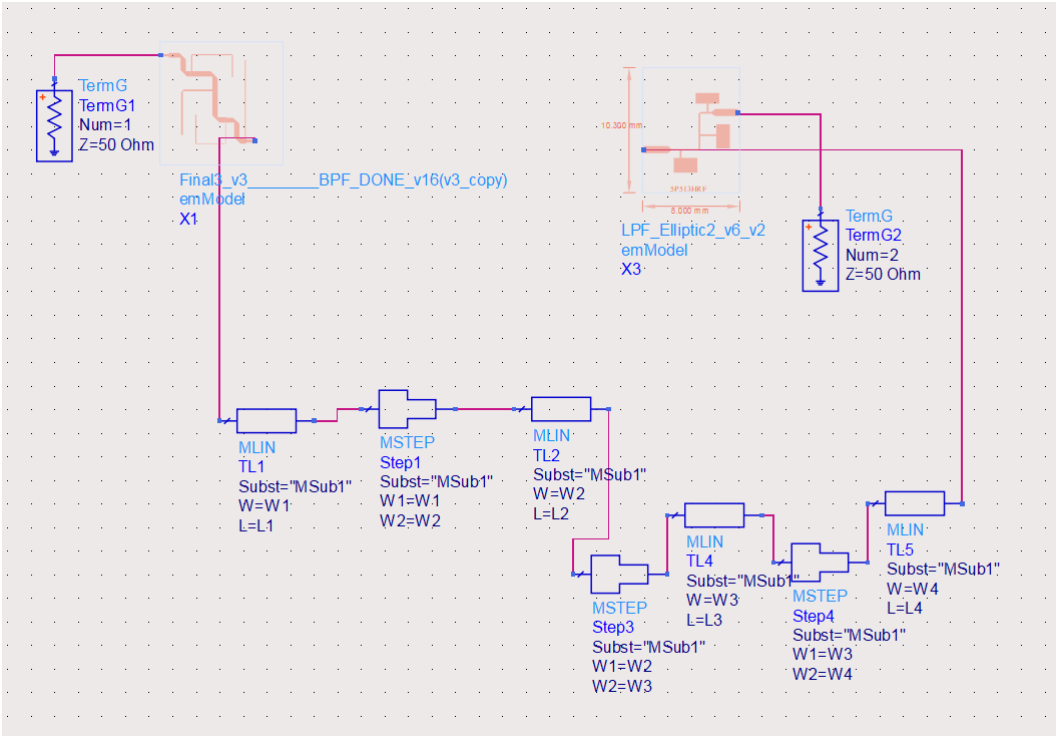

Figure 3.28 Co-simulation for impedance matching using stepped impedance network

Co-Simulation 2 Response:

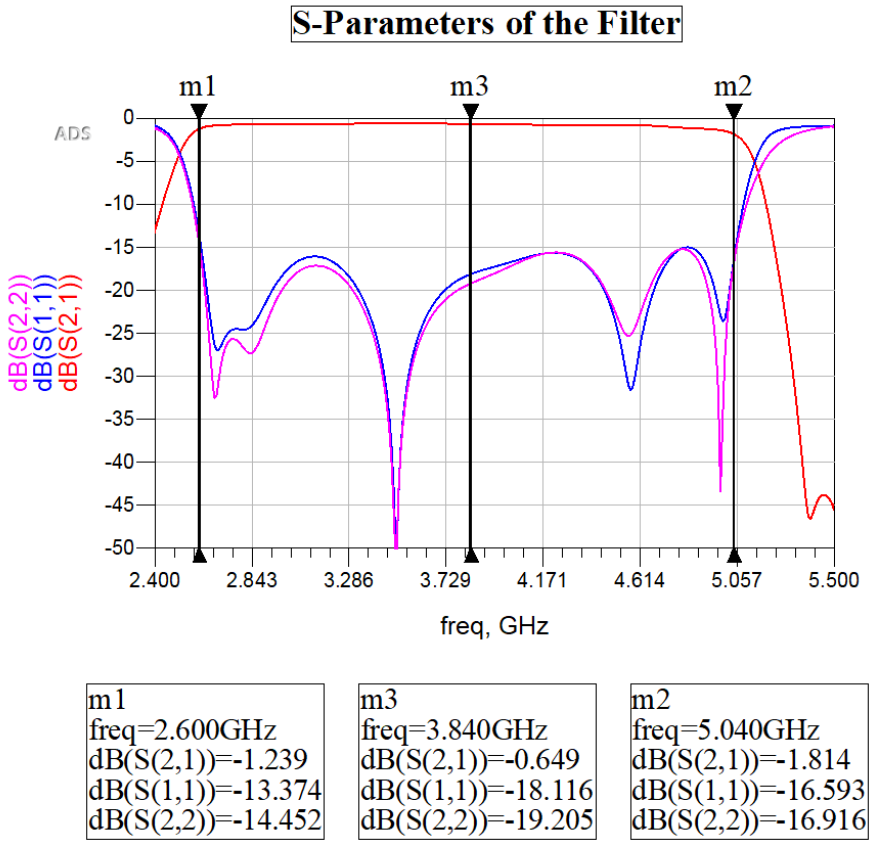

Figure 3.29 S-Parameters from co-simulation 2

Both the impedance matching networks shows promising result and can be utilised, however both fails to satisfy the substrate area constraint, because of which a simple micro strip line of 10 mm length and 0.6 mm thick is connected in-between the two filters, which also shows somewhat similar response.

CHAPTER-4 FINAL PROPOSED DESIGN

After performing several iterations regarding the design of both the BPF and HRF in the previous chapter along with the impedance matching between the two. This chapter contains the final proposed integrated design of the filter.

4.1 Layout Design Without Tuning Pads

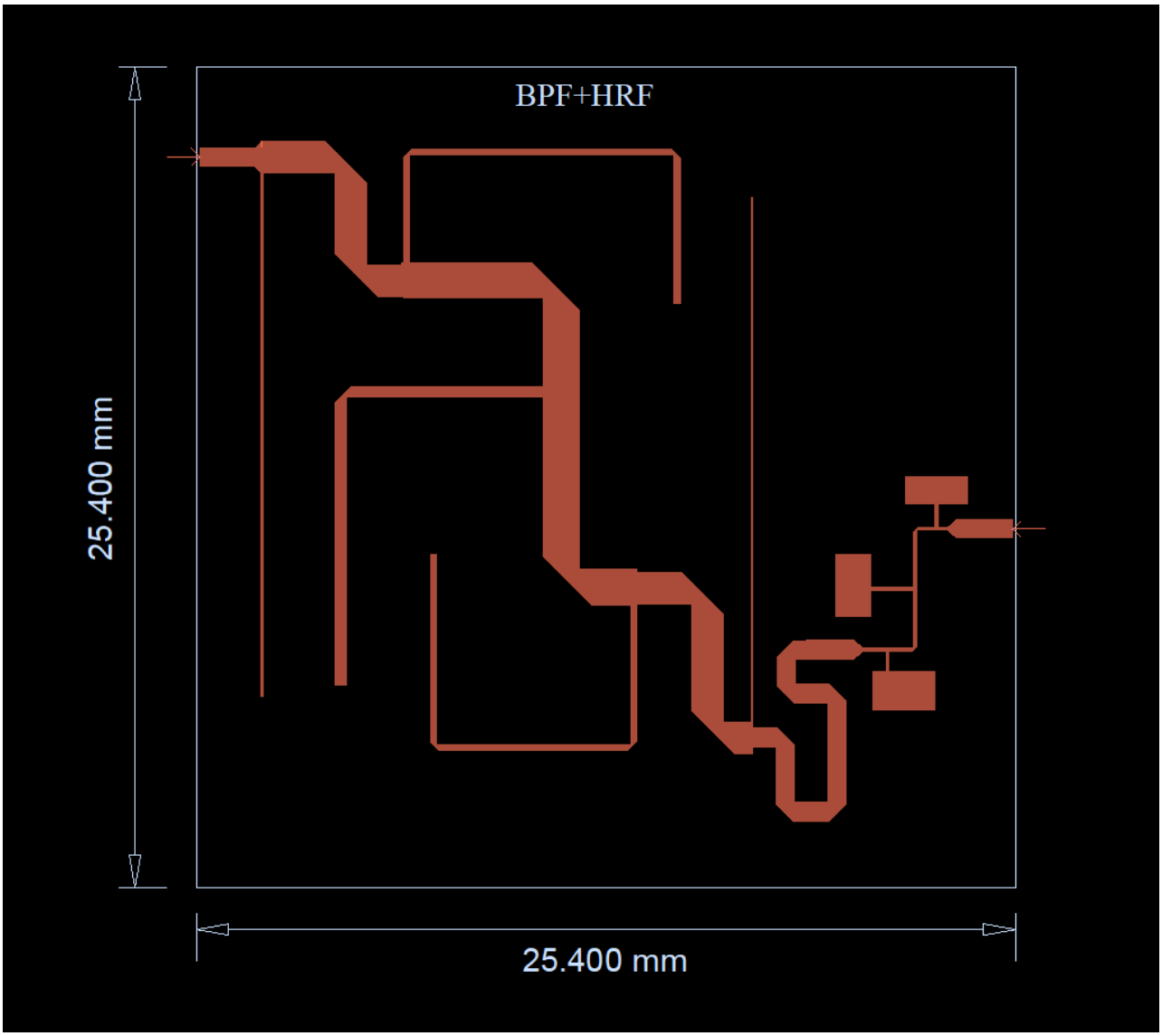

Figure 4.1 Final proposed layout (BPF+HRF)

The above shown layout is the final proposed layout that actually satisfies the specification mentioned along with the fixing of the issue because of open-stub topology. However, for practical testing purposes there is requirement of adjusting the lines' properties, the next design shows contains the tuning pads that are required for further manual tuning for testing purpose.

4.2 Layout Design With Tuning Pads

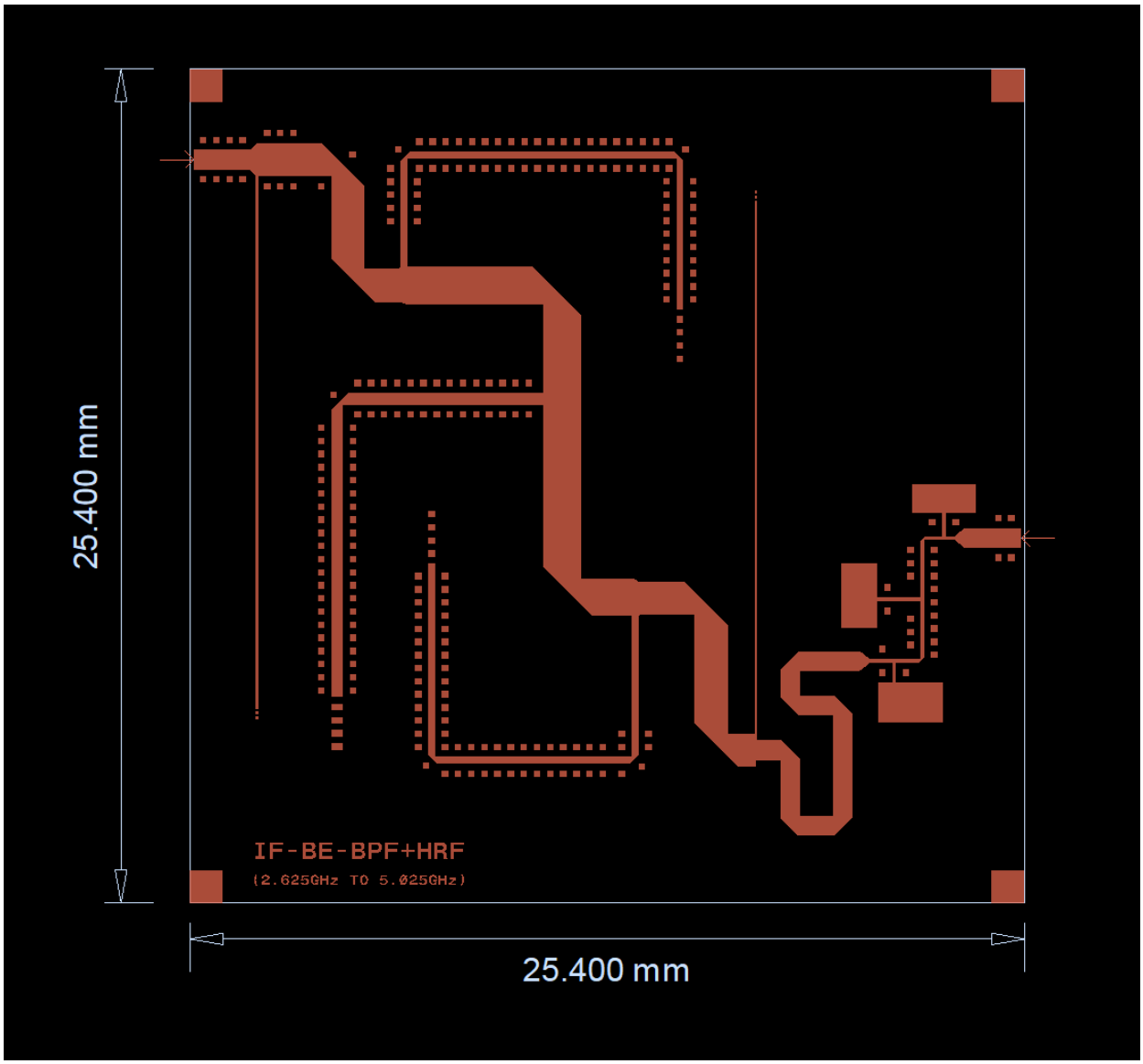

Figure 4.2 Final proposed layout with tuning pads (BPF+HRF)

The simulated S-Parameters of the above layout is shown on the next page.

4.3 Layout Simulation Results

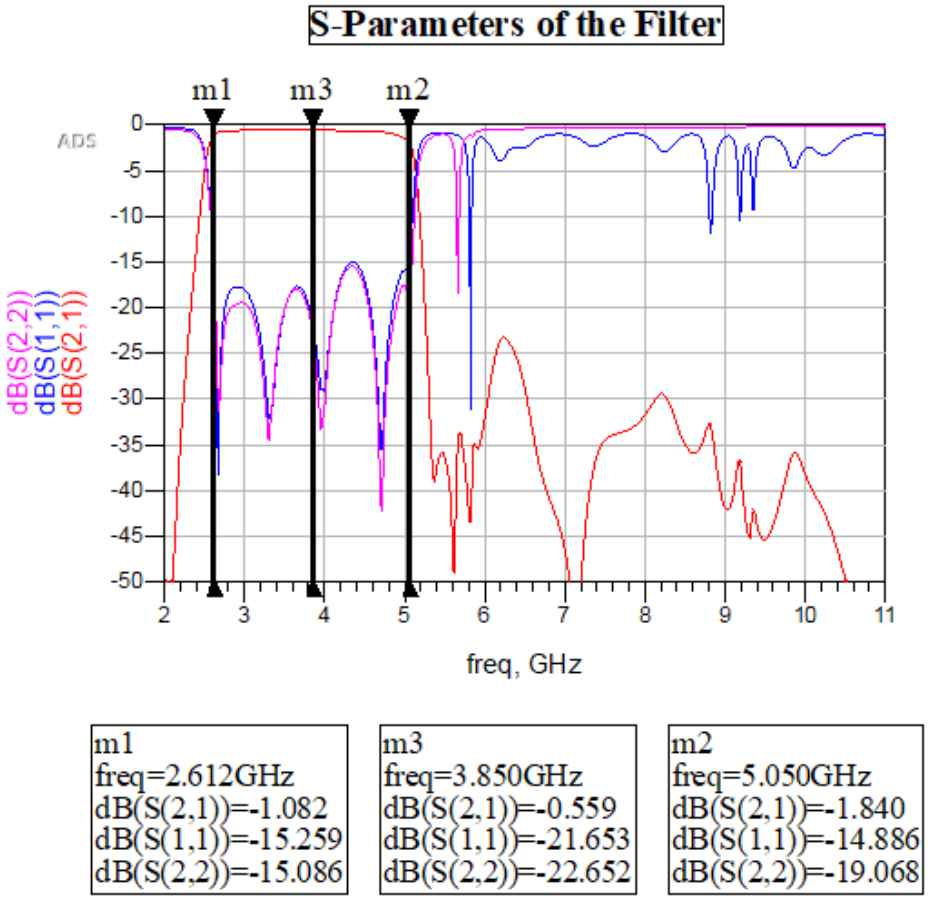

Figure 4.3 S-Parameters from layout simulation

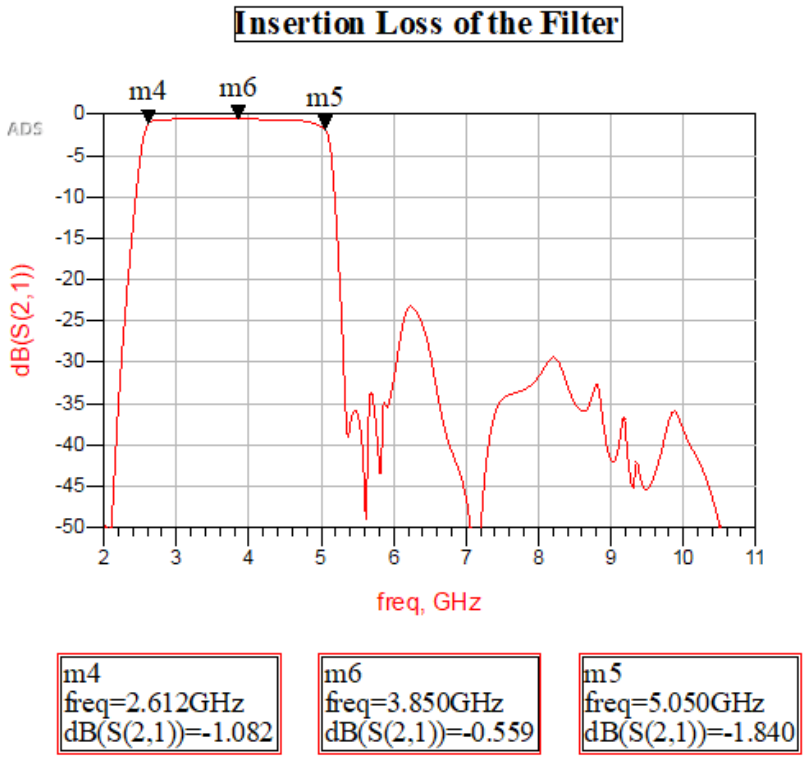

Figure 4.4 Insertion loss of the filter

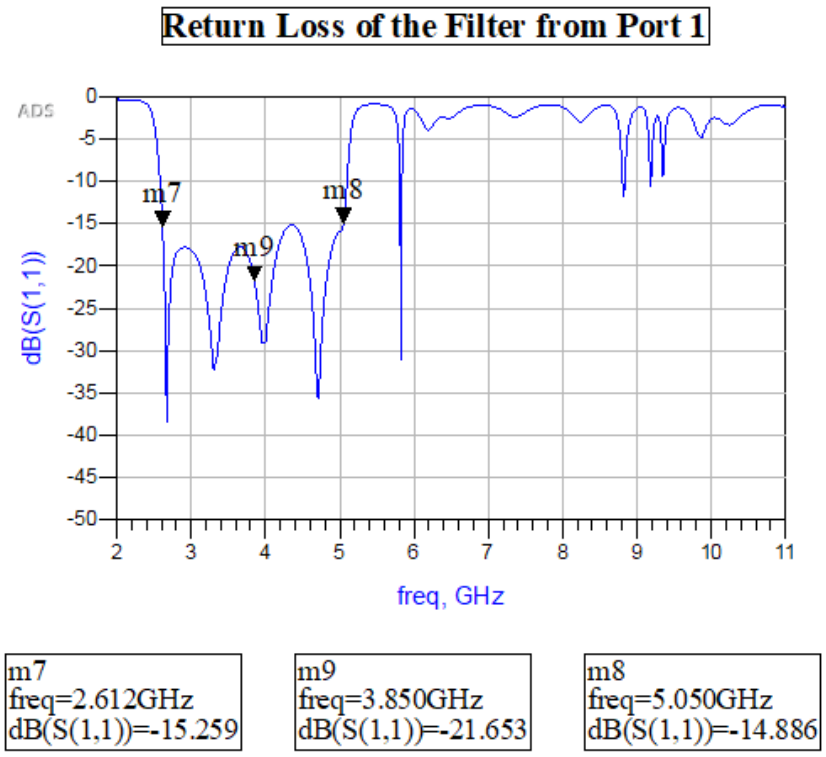

Figure 4.5 Return loss of port 1

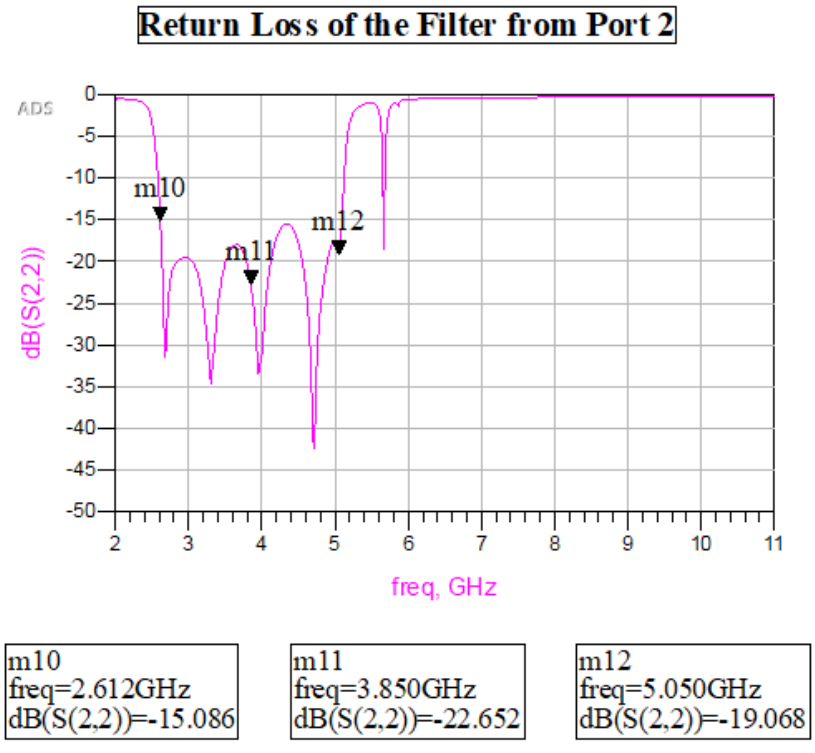

Figure 4.6 Return Loss of port 2

Observation: The simulated result shows the elimination of the extra passband (harmonic) along with a better return loss than the specified return loss for most of the passband.

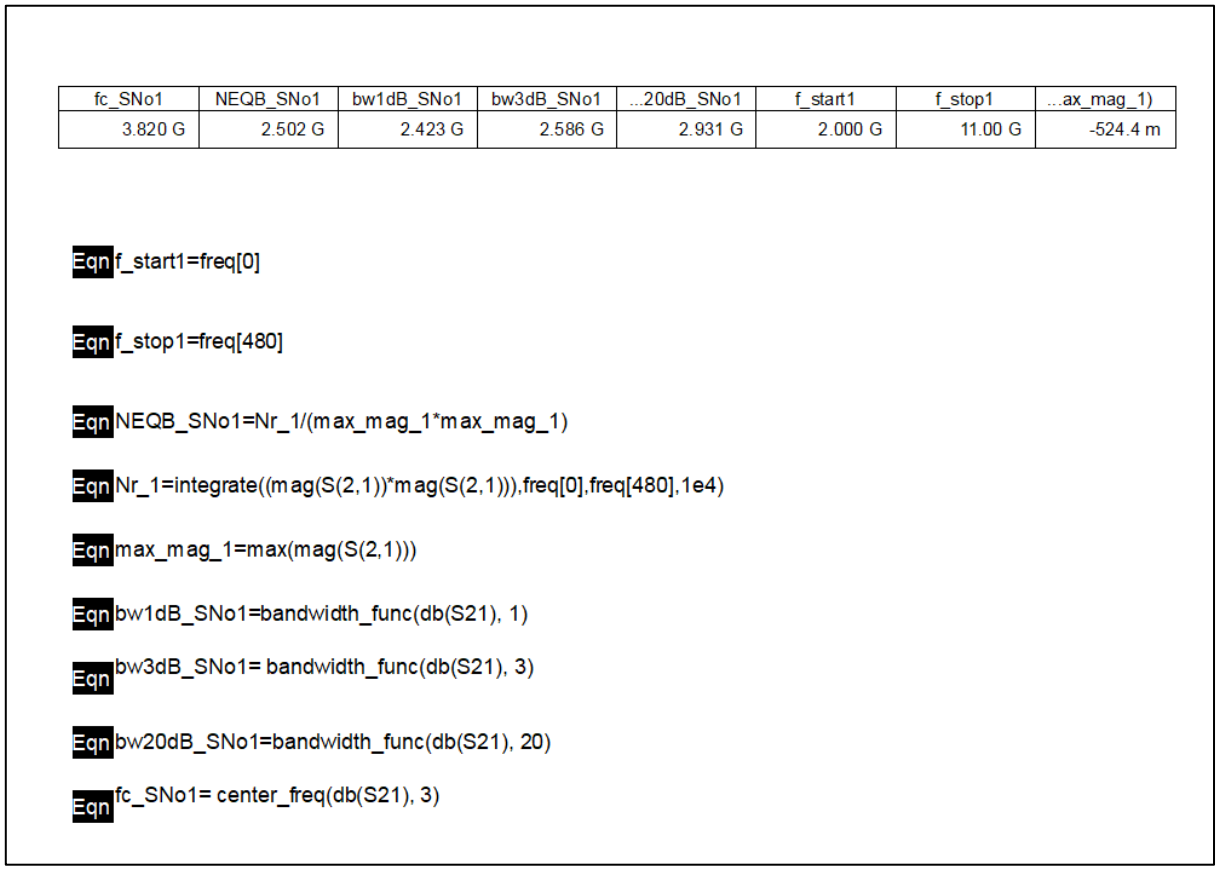

fc_SNo1	NEQB_SNo1	bw1dB_SNo1	bw3dB_SNo1	...20dB_SNo1	f_start1	f_stop1	...ax_mag_1)
3.820 G	2.502 G	2.423 G	2.586 G	2.931 G	2.000 G	11.00 G	-524.4 m

Eqn f_start1=freq[0]

Eqn f_stop1=freq[480]

Eqn NEQB_SNo1=Nr_1/(max_mag_1*max_mag_1)

Eqn Nr_1=integrate((mag(S(2,1))*mag(S(2,1))),freq[0],freq[480],1e4)

Eqn max_mag_1=max(mag(S(2,1)))

Eqn bw1dB_SNo1=bandwidth_func(db(S21), 1)

Eqn bw3dB_SNo1= bandwidth_func(db(S21), 3)

Eqn bw20dB_SNo1=bandwidth_func(db(S21), 20)

Eqn fc_SNo1= center_freq(db(S21), 3)

Figure 4.7 Noise equivalent bandwidth calculation

Conclusion: The proposed design successfully satisfies the required specifications along with physical size constraints and is ready for practical testing.

CONCLUSION

The purpose of the report is to provide an in-depth procedure driven approach into designing of ultra-wideband micro strip Band pass filter. The discussion first starts with basic theoretical concepts that are needed to be done in a brief before starting with the designing purpose. Thereafter, the entire design process starts from basic equations and a theoretical approach after which the practical designing is started. It is to be noted that the exact theoretical approach did not give the expected response when converted to the practical design. This might be due to the fact of making some assumptions for some filter specifications and using a set of different normalised prototype component values than that of the expected values.

Final design consists of a 5^{th} order open-stub Band Pass Filter satisfying the specifications. However, to mitigate the adverse effect of the open-stub topology i.e. existence of harmonics beyond both lower and upper passband limits, a Harmonic Rejection Filter (HRF) is also designed. At the end both the filters are cascaded into a single 1-inch square substrate.

The measured response of the final proposed layout design gives a passband of 2.612GHz to 5.050 GHz covering a total bandwidth of 2.438GHz (2.44 GHz approx..). The extra limit is considered due to the fact of possible shrinkage of +-8 um while fabrication procedure. The insertion loss maintains a value < 2dB with the maximum value of 1.840 dB at 5.050 GHz. The return losses from both port 1 and 2 are recorded with the minimum return loss of 15 dB satisfying the specification.

The Noise Equivalent Bandwidth is calculated at the end, recorded as 2.502 GHz (within +-10% limit), also satisfying the required specification.

A final simulation is done where the frequency value is varied from 0.075 – 17.25 GHz, beyond 14.3 GHz and till ____ there is certain peak in the response which ultimately increases the Noise Equivalent Bandwidth upto 2.802 GHz.

SCOPE OF FUTURE WORK

The design can further be optimised to make sharper roll-off and better return loss. It is to be noted that the actual frequency range the filter is exposed to is from 0. 075 GHz to 11 GHz, but due to the existence of harmonic beyond the lower passband limit, the exact requirement is not met. This can be mitigated using two options, first is the actual testing of the filter and checking whether the actual range starts from what is considered in the simulation results. Second, to design a small HPF with a 3dB cut-off frequency around 1.85 GHz.

The HPF design must not be done on the same substrate as of the current design, as the substrate used in this design does not supports the creation of vias or presence of any short-circuit element. It can be done by bringing the ground connection to the edge of the carrier plate (CP), which might make it difficult to get fitted into the same substrate area.

The solution for the sudden peak in the response at 14.5 GHz can be solved using two options, either by implementing the same HRF again cascaded with the existing design or can be mitigated by a quarter-wave stub connection.

REFERENCES

[1] Yousefi, Mohammad, Hadi Aliakbarian, and Ramezanali Sadeghzadeh. "Design and integration of a high-order hairpin bandpass filter with a spurious suppression circuit." In 2015 Loughborough Antennas & Propagation Conference (LAPC), pp. 1-4. IEEE, 2015.

[2] Mirete, Takele Yonas, Gebre Fisehatsion Mesfin, Meresa Girma Nigus, Tegegne Solomon Eshetie, Mengesha Yared Getachew, and Molla Eldana Beyene. "Design of 2-12 GHz ultra-wideband band pass filter using GAAS integrated passive device technology." In 2022 19th International Computer Conference on Wavelet Active Media Technology and Information Processing (ICCWAMTIP), pp. 1-5. IEEE, 2022.

[3] Kanaparthi, V. Phani Kumar, Vamsi Krishna Velidi, and Rengasamy Rajkumar. "A compact ultra-wideband multimode bandpass filter with sharp-rejection using stepped impedance open stub and series transformers." IEEE Transactions on Circuits and Systems II: Express Briefs 69, no. 12 (2022): 4824-4828.

[4] Sarkar, Mahadev. "Sharp Rejection Wideband Band Pass Filter in Suspended Substrate Stripline Realization." In 2019 IEEE 5th International Conference for Convergence in Technology (I2CT), pp. 1-6. IEEE, 2019.

[5] He Zhu, Qing-Xin Chu. “Ultra-wideband (UWB) bandpass filter with sharp selectivity and wide upper stopband” ICUWB 2012.

[6] Jia-Sheng Hong, M.J.Lancaster. “Microstrip Filters for RF/Microwave Applications”.

[7] David M. Pozar. “Microwave Engineering”, 4th Edition.

[8] T.C Edwards, M.B Steer. “Foundations of Interconnect and Microstrip Design”, 3rd Edition.